



Marked spatiotemporal variations in small phytoplankton structure in contrasted waters of the Southern Ocean (Kerguelen area)

Solène Irion ^{1,*} Ludwig Jardillier ² Ingrid Sassenhagen,¹ Urania Christaki¹

¹Laboratoire d'Océanologie et de Géosciences, UMR 8187, Université du Littoral Côte d'Opale, CNRS, Université de Lille, Wimereux, France

²Unité d'Ecologie, Systématique et Evolution, Université Paris-Sud, CNRS, AgroParisTech, Université Paris-Saclay, Orsay Cedex, France

Abstract

In the Southern Ocean, diatom blooms have attracted a lot of attention, while other small nonsilicified phytoplankton groups have been less studied. Here, small phytoplankton (< 20 μm , including small diatoms and nonsilicified small phytoplankton) are focused on in two contrasting areas: the productive Kerguelen plateau and its surrounding low productivity waters. To assess the diversity and spatial structuration of phytoplankton, discrete plankton samples (0–300 m layer) of two size fractions (< 20 and 20–100 μm) were analyzed with 18S rDNA amplicon sequencing in late summer. Phytoplankton seasonal succession was described using flow cytometry, pigments, and environmental data, from two previous cruises (during the onset and decline of the diatom bloom). In the mixed layer, small nonsilicified phytoplankton represented less than 10% of chlorophyll *a* (Chl *a*) during the onset and late diatom bloom on the plateau, but they increased on and off the plateau after the bloom (53–70% of Chl *a*). *Phaeocystis antarctica* was relatively abundant at all stations after the bloom, but other small phytoplanktonic groups featured marked differences on and off the plateau. Higher NH_4^+ concentrations on the plateau appeared to stimulate the presence of *Micromonas*, while Pelagophytes were enhanced off the plateau. A diverse assemblage of small diatoms was also promoted off the plateau, where silicate concentration was still high. Interestingly, *P. antarctica* represented up to 25% of all reads at 300 m depth off the plateau in the larger size fraction suggesting a significant contribution to carbon export through aggregation in low productive waters.

Small phytoplankton (< 20 μm) play key roles in the global carbon cycle and marine food webs (Marañón et al. 2001; Richardson and Jackson 2007; Uitz et al. 2010). Typically, small phytoplankton have an advantage over larger cells in nutrient uptake due to their higher surface to volume ratio (Chisholm 1992; Agawin et al. 2000; Irwin et al. 2006). The Southern Ocean (SO) is the earth's largest high nutrient low chlorophyll (HNLC) area where phytoplankton production is limited by iron despite high concentrations of macronutrients, such as nitrate, silicate, or phosphate (Martin 1990; de Baar et al. 1995). Phytoplankton in these low productive HNLC waters is typically composed of small cells (< 20 μm), including small nonsilicified phytoplankton and diatoms (Moore

and Abbott 2000; Kopczynska et al. 2001; Uitz et al. 2009, 2010; Lasbleiz et al. 2014). Here, annual primary production of small phytoplankton collectively exceeds the large phytoplankton (herein defined as large-size cells, > 20 μm) by a factor of 2.7 (2.5 Gt C yr⁻¹ and 0.9 Gt C yr⁻¹, respectively; Uitz et al. 2010). Despite their significant functional role, their diversity and spatiotemporal dynamics have remained overlooked in the SO (e.g., Weber and El-Sayed 1987; Wright et al. 2009; García-Muñoz et al. 2013), when large diatom blooms and the classical Antarctic food chain (diatoms–krill–whales) have received much more attention.

In contrast to HNLC low productive waters, discrete areas of the SO naturally, fertilized in iron and highly productive, are characterized by large diatoms bloom from spring to summer (Blain et al. 2007; Korb et al. 2008; Pollard et al. 2009). This is the case south-east of the Kerguelen archipelago where large diatom blooms appear at this time and result in a chlorophyll-rich area of 45,000 km², constrained by the bathymetry of the plateau (Blain et al. 2007; Mongin et al. 2008). Upward fluxes of deep iron and major nutrients from the shallow continental shelf of the Kerguelen plateau

*Correspondence: solene.irion@univ-littoral.fr

This is an open access article under the terms of the Creative Commons Attribution License, which permits use, distribution and reproduction in any medium, provided the original work is properly cited.

Additional Supporting Information may be found in the online version of this article.

(< 500 m) sustain these blooms (Blain et al. 2007; Mongin et al. 2008; Park et al. 2008). The blooms over the plateau can be dominated either by small diatoms forming long chains (chain length > 100 μm , e.g., *Pseudo-nitzschia*, *Chaetoceros*) or large diatoms (*Eucampia*, *Corethron*). In contrast, small phytoplankton (mostly *Phaeocystis* and small diatoms) dominates in surrounding HNLC waters and production remains low throughout the year (Fiala et al. 1998; Kopczyńska et al. 1998; Armand et al. 2008; Uitz et al. 2009; Lasbleiz et al. 2016).

Community composition, temporal succession, and contribution to carbon export of diatoms during their blooming period around Kerguelen are well documented (Armand et al. 2008; Rembauville et al. 2015, 2017, 2018; Lasbleiz et al. 2016). Previous cruises KEOPS 1 and 2 (Kerguelen Ocean and Plateau compared Study project) investigated phytoplankton composition and C-cycling during the onset and decline of the bloom. The carbon export efficiency during the onset and decline of the bloom was lower on the plateau than in the HNLC area (e.g., Christaki et al. 2014; Laurenceau-Cornec et al. 2015; Planchon et al. 2015) although the amount of carbon exported at 200 m was twofold higher on the plateau (Blain et al. 2007; Planchon et al. 2015). At a broader scale, this inverse relationship between production and export seems to be a feature of the SO (Maiti et al. 2013; Le Moigne et al. 2016). This pattern could be explained by differences in phytoplankton communities (dominance of either small or large cells) and resulting trophic structures, grazing intensity, and/or microbial mineralization (Maiti et al. 2013; Laurenceau-Cornec et al. 2015; Le Moigne et al. 2016).

As chain-forming and large-diatom blooms occur during relatively short periods, it has been hypothesized that small-size cells are an essential element of Antarctic food webs, especially during winter and periods preceding blooms (Detmer and Bathmann 1997). Satellite data and sampling has indicated that phytoplankton communities on the plateau switch to an ecosystem dominated by small phytoplankton before (Rembauville et al. 2017), and also likely, after the bloom (Penna et al. 2018). As such, the plateau of Kerguelen could also include a persistent and functionally important small phytoplankton community, on which diatom blooms superimpose themselves (Smetacek et al. 1990).

Despite their ecological importance, little is known about the diversity, spatiotemporal dynamics, and environmental drivers of small phytoplankton in the SO. *Phaeocystis antarctica* has been identified as a putative key player in the absence of diatom blooms (Froneman et al. 2004; Hashihama et al. 2008; Iida and Odate 2014; Schulz et al. 2018). Early molecular studies specifically targeting Antarctic small plankton used technologies such as clone libraries or molecular fingerprinting techniques (Díez et al. 2001; Díez et al. 2004; Gast et al. 2004; Piquet et al. 2011). These technologies were unable to depict the full microbial diversity that is dominated by low-abundant taxa (Pedròs-Alio 2007). High-

throughput sequencing of size fractionated samples allowed further description of the diversity of small microbial eukaryotes (Wolf et al. 2014; Clarke and Deagle 2018). However, summer to autumn transition (March) and winter have not been investigated thus far, although these are the periods when the ecosystem most likely relies on primary production by small phytoplankton. Moreover, phytoplankton seasonal dynamics around the Kerguelen Islands has not been fully described yet.

The MOBYDICK (Marine Ecosystem Biodiversity and Dynamics of Carbon) cruise took place in late February and March 2018, a month after the diatom bloom ended. MOBYDICK's two main objectives were: to trace carbon from its initial fixation at the surface to its final export toward the ocean interior, and to explore how diversity influenced the carbon cycle in contrasted marine ecosystems on and off the iron enriched waters of the Kerguelen plateau. The present study focuses on the composition, seasonal variability, and ecology of small phytoplankton on and off the plateau. Molecular diversity of microbial eukaryotes after the bloom (MOBYDICK) is described through 18S rDNA amplicon Illumina Mi-Seq sequencing of small and large-cells size fractions (< 20 and 20–100 μm). Pigment and flow cytometry data from two previous cruises at the early and late stage of the bloom (KEOPS2 and KEOPS 1, respectively) were also used to complete the seasonal succession of phytoplankton on and off the plateau of Kerguelen. Environmental factors likely governing the balance between small phytoplankton vs. large diatoms throughout the season and potential ecological implications for carbon export are also identified.

Materials and methods

Sampling strategy overview

Seawater was collected onboard the R/V *Marion Dufresne* around the plateau of Kerguelen Islands during the MOBYDICK cruise after the diatom bloom (26 February 2018–18 March 2018). We combined samples from the MOBYDICK cruise with data collected during past cruises undertaken at different seasons to describe the seasonal succession. To do so, we restricted the pigment and cytometry data to a similar depth horizon (upper 50 m) and to stations presenting either the same location on the plateau and reference station in the HNLC area off the plateau. KEOPS2 cruise took place during austral spring (15 October 2011–20 November 2011), while KEOPS1 occurred during summer (19 January 2005–13 February 2005) (Table 1). Plateau Sta. A3 of KEOPS1 and 2 corresponds to MOBYDICK Sta. M2 (Fig. 1). This station experiences natural iron enrichment from the plateau resulting in diatom blooms during spring and early summer (Armand et al. 2008; Lasbleiz et al. 2016). Off-plateau stations M1, M3, and M4 (MOBYDICK) were expected to

display HNLC characteristics. Sta. R-2 (KEOPS2) and Sta. C11 (KEOPS1) were the HNLC reference stations (Quéguiner et al. 2007; Cavagna et al. 2015), which will be considered here for the seasonal succession (Fig. 1; Table 1).

Environmental parameters

For KEOPS 1 and 2, environmental parameters were described in Mosseri et al. (2008) and Cavagna et al. (2015). For MOBYDICK, temperature, dissolved oxygen, and salinity measurements were collected at all CTD casts using a SeaBird 911-plus.

Table 1. Coordinates and dates of samples collected during KEOPS 1 and 2 and MOBYDICK.

| Cruise | Station | Date | Longitude (°E)* | Latitude (°S)* |
|---------|-----------|-----------|-----------------|----------------|
| KEOPS 2 | A3-1 | 20 Oct 12 | 72.1 | 50.6 |
| | R2 | 26 Oct 12 | 66.7 | 50.4 |
| | A3-2 | 16 Nov 12 | 72.1 | 50.6 |
| KEOPS 1 | A3-1 | 19 Jan 05 | 72.0 | 50.4 |
| | A3-2 | 23 Jan 05 | 72.0 | 50.4 |
| | C11-1 | 26 Jan 05 | 77.6 | 51.4 |
| | C11-2 | 28 Jan 05 | 77.6 | 51.4 |
| | A3-3 | 04 Feb 05 | 72.0 | 50.4 |
| | A3-4 | 12 Feb 05 | 72.0 <td 50.4 | |
| | MOBYDICK | M2-1 | 26 Feb 18 | 72.0 |
| M2-2 | 06 Mar 18 | 72.0 | 50.4 | |
| M2-3 | 16 Mar 18 | 72.0 | 50.5 | |
| M1 | 09 Mar 18 | 74.5 | 49.5 | |
| M3-1 | 04 Mar 18 | 68.0 | 50.4 | |
| M3-3 | 19 Mar 18 | 68.0 | 50.4 | |
| M4-1 | 01 Mar 18 | 67.1 | 52.4 | |
| M4-2 | 13 Mar 18 | 67.1 | 52.4 | |

*Coordinates and depth of the CTD “stock.”

Ammonium was measured by fluorometry (Holmes et al. 1999). For other dissolved inorganic nutrients (PO_4^{3-} , $\text{Si}(\text{OH})_4$, NO_2^- , NO_3^-), samples were collected in 125 mL polyethylene bottles. The samples were then filtered through $0.45 \mu\text{m}$ acetate cellulose filters and preserved with $100 \mu\text{L}$ HgCl_2 (4 g L^{-1}) in 20 mL. The samples were then stored in the dark at room temperature until analysis in the laboratory with a segmented flow analyzer (Skalar) equipped with colorimetric detection using methods described in Aminot and K erouel (2007).

Sample collection for DNA extraction and molecular biology

During the MOBYDICK cruise, four different sites were visited. M2, located on the plateau, was sampled three times during the cruise with about a 10-d interval. Off the plateau, M3 and M4 were sampled twice with a 2-weeks interval, and M1 only once (Table 2). Seawater samples were collected with 12-liter Niskin bottles at all visited stations at four depths (15, 60, 125, and 300 m). The first two depths (15 and 60 m) were chosen to correspond approximately to the surface and bottom of the mixed layer (ML), respectively. Water at 300 m was characteristic of deep nutrient-rich winter water (Park et al. 2008). Water at 125 m corresponded to the “transition layer,” defined as the water mass at the interface between the deep stratified ocean interior and the highly turbulent surface ML (Johnston and Rudnick 2009).

Sampled seawater was first prefiltered using a $100 \mu\text{m}$ nylon mesh (Millipore, U.S.A.) in order to remove Metazoa and large particles. Ten liters of water from each depth were then filtered successively through 20 and $0.2 \mu\text{m}$ pore-size membranes (Millipore) for microbial eukaryote taxonomic composition analyses of large ($100\text{--}20 \mu\text{m}$) and small size-fractions ($< 20 \mu\text{m}$). This resulted in 64 samples (eight visits at the different stations, four depths, two size fractions). Filters were directly frozen and stored at -80°C for 18S rDNA

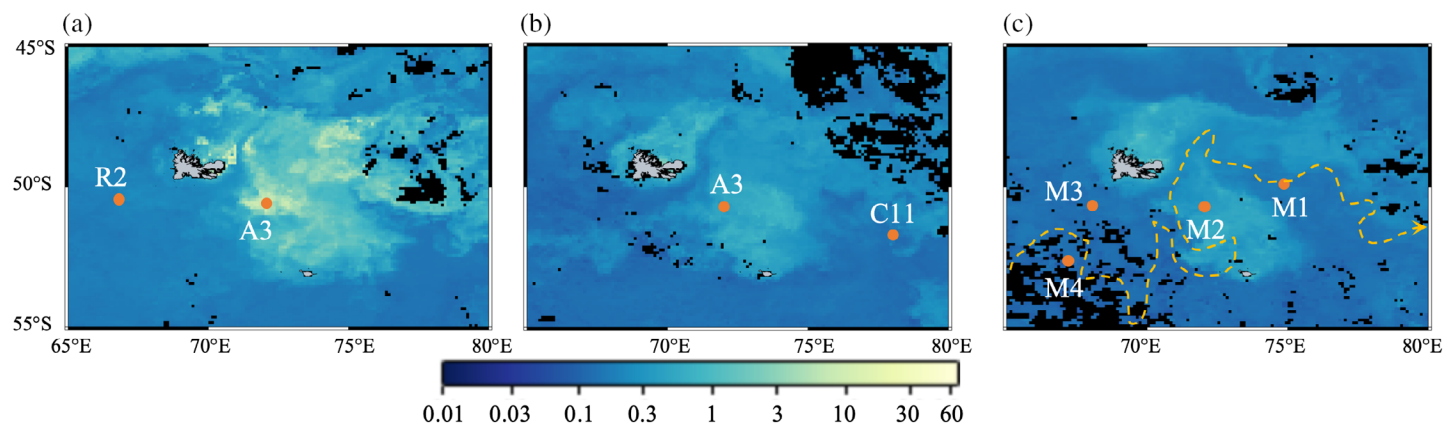


Fig. 1. Location of plateau and off-plateau reference stations sampled during KEOPS2 (a), KEOPS1 (b), and MOBYDICK (c). Chl *a* (color scale) represented on the map corresponds to AQUA/MODIS average values ($\mu\text{g L}^{-1}$) over the respective cruises’ sampling periods (November 2011 for KEOPS2, January and February 2005 for KEOPS1, and March 2018 for MOBYDICK). The dotted yellow line represents the position of the Polar Front in March 2018 according to Pauthenet et al. (2018).

Table 2. Description of MOBYDICK stations. The depth of the mixed layer (ZML) is based on a difference in sigma of 0.02 compared to surface value. The mean ZML is calculated based on all CTD casts performed during the occupation of the stations. Temperature, nutrients, and Chl *a* are mean values of all measures sampled within the ML (2–3 depths depending on the station). The depth of the euphotic layer (Ze) corresponds to the depth where light intensity was at least 1% of incident light at surface during the CTD cast of the sampling for metabarcoding.

| Station | Date | Depth (m) | <i>T</i> (°C) | ZML (m) | Ze (m) | Chl <i>a</i> (μg L ⁻¹) | NO ₃ ⁻ + NO ₂ ⁻ (μmol L ⁻¹) | NH ₄ ⁺ (μmol L ⁻¹) | PO ₄ ³⁻ (μmol L ⁻¹) | Si(OH) ₄ (μmol L ⁻¹) |
|---------|--------------|-----------|---------------|---------|--------|------------------------------------|---|--|---|---|
| M2-1 | 26 Feb 18 | 520 | 5.10 | 62 | 45 | 0.27 | 21.90 | 0.75 | 1.47 | 1.36 |
| M2-2 | 06 Mar 18 | 519 | 5.24 | 61 | 46 | 0.30 | 21.79 | 1.1 | 1.50 | 1.72 |
| M2-3 | 16 Mar 18 | 527 | 5.11 | 68 | 45 | 0.58 | 21.90 | 0.94 | 1.50 | 2.75 |
| M1 | 09 Mar 18 | 2723 | 4.99 | 27 | 56 | 0.35 | 25.20 | 0.56 | 1.71 | 8.38 |
| M3-1 | 04 Mar 18 | 1730 | 5.6 | 65 | 75 | 0.20 | 23.75 | 0.50 | 1.65 | 2.89 |
| M3-3 | 19 Mar 18 | 1730 | 5.31 | 79 | 62 | 0.14 | 23.34 | 0.73 | 1.08 | 2.31 |
| M4-1 | 01 Mar 18 | 4186 | 4.45 | 49 | 66 | 0.18 | 25.70 | 0.37 | 1.70 | 4.36 |
| M4-2 | 13 Mar 18 | 4300 | 4.46 | 87 | 64 | 0.21 | 24.80 | 0.48 | 1.71 | 4.80 |

amplicon Illumina Mi-Seq sequencing. Each filter was cut into small pieces before DNA extraction with PowerSoil DNA Isolation Kit (QIAGEN, Germany) following standard manufacturer's protocol. DNA was eluted with 100 μL AE buffer.

Polymerase chain reaction and Illumina sequencing

To describe protist diversity, the V4 hypervariable region of the 18S rRNA gene was amplified using the primers EK-565F (5'-GCAGTAAAAAGCTCGTAGT) and UNonMet (5'-TTTAA GTTTCAGCCTTGCG) biased against Metazoa (Bower et al. 2004). Different molecular identifiers of 10 bp were added to both forward and reverse primers to tag amplicons and allow to differentiate them after sequencing. Polymerase chain reaction (PCR) mixtures comprised 1–2 μL of DNA, 12.5 μL of DreamTaq Green PCR Master Mix (Thermo Fisher Scientific, U.S.A.), and 1 μL of each primer (10 μmol L⁻¹) in a total volume of 25 μL. PCR conditions included an initial step of denaturation at 94°C for 3 min, 25 cycles of denaturation at 94°C for 30 s, annealing at 58°C for 45 s, and extension at 72°C for 90 s, and a final step of extension at 72°C for 10 min. PCR products from at least five different PCR reactions of each sample were then pooled together and purified using the QIAquick PCR purification kit (QIAGEN, Germany), according to the manufacturer's instructions. DNA concentrations were calculated on a Qubit fluorometer with the dsDNA High Sensitivity Assay Kit (Life Technologies Corp., U.S.A.) and identical concentrations of each sample's amplicons were pooled.

Pooled amplicons were then paired-end sequenced on an Illumina MiSeq 2 × 300 platform by Genewiz (U.S.A.).

Demultiplexing, quality filtering, and taxonomic affiliation

Paired-end sequences were imported and demultiplexed in Qiime (Caporaso et al. 2010) based on each sample's 10 bp molecular identifier with the functions `extract_barcodes.py` (Qiime1) and `demux emp-paired` (Qiime 2-2018.8). Demultiplexed sequences without primers and barcodes were further processed in R-software (R Core Team 2018) using the DADA2 package v.1.10.1 (Callahan et al. 2016) to define amplicon sequence variants (ASVs). Sequences were quality filtered (maximum expected error = 6), trimmed (forward and reverse reads at 270 nt) prior to inferring ASVs and removing chimeric sequences with the DADA2 algorithm. Taxonomy was assigned for each ASV to the best taxonomic level using the RDP naive Bayesian classifier implemented in DADA2 (Wang et al. 2007) in combination with PR² database v.4.11.0 (Guillou et al. 2013), a curated database implementing EukRef (del Campo et al. 2018). Taxonomy assigned this way was cross-checked with Sintax algorithm in USEARCH v11 (Edgar 2013). When taxonomy assignment differed between the two algorithms, taxonomy was compared to NCBI blast and/or limited to the highest taxonomic level where both algorithms agreed. All ASVs sequences were aligned in Geneious Prime v.2019 using MAFFT v7.388 plugin (Katoh and Standley 2013) parameterized for FFT-NS-2 analysis to

deal with the large number of sequences. A phylogenetic tree was then built based on this alignment with FastTree 2.1.5 plugin using default parameters (Price et al. 2009). All data for this study are accessible in the MOBYDICK database (<http://www.obs-vlfr.fr/proof/php/mobydick/mobydick.php#SA>). Raw sequencing files in fastq format, as well as ASVs, taxonomy and metadata tables are available at http://www.obs-vlfr.fr/proof/ftppfree/mobydick/db/DATA/PAR_2251/.

Statistical analysis

Alpha diversity analyses were conducted in R-software version 3.5.1 (R Core Team 2018) on ASVs with phyloseq v.1.16 (McMurdie and Holmes 2013) and microbiomeSeq (Ssekagiri et al. 2018) after rarefying read depths based on sample with the lowest read count. Observed richness and Pielou's evenness (i.e., $J = H'/\ln[S]$ where H' is Shannon Weiner diversity index and S is the total number of species in a sample indexes) were compared between size fractions and locations with ANOVA, followed by pairwise tests using Tukey multiple comparisons (Tukey's honestly significant difference test) with 95% confidence interval.

To illustrate community composition differences between samples, phyloseq was used to plot PCoA based on weighted UniFrac distances, that considers the phylogenetic distance between two sample's composition and ASVs relative abundances (Lozupone et al. 2011). Cluster analysis was conducted based on the wUniFrac distance matrix using the hclust function in R-software and Ward classification method (Murtagh and Legendre 2014). Homogeneity of dispersion (variance) within group was calculated with function betadisperser. ANOVA-like test (permutest) was used to determine if the variances differed by groups.

Heatmaps of the 30 most abundant genera were generated using "Ampvis2" R-package (Andersen et al. 2018) after pooling ASVs belonging to the same genus. To test for statistical differences in community composition according to a variable of interest (size fraction, location of the station on or off the plateau), permutational analysis of variance (PERMANOVA) implemented in the function adonis from the "vegan" R-package (Oksanen et al. 2017) was run on weighted UniFrac distances with 1000 permutations. To identify genera differing in abundance between plateau and off-plateau surface samples (10 and 60 m), un-normalized table of ASVs, pooled by genus when possible, representing over 1% of the reads, were transformed using DESeq2 (v1.22.2) (Love et al. 2014). The same package was used to perform the differential analysis. All genera that were significantly different in abundance between plateau and off-plateau surface samples (p value, adjusted for multiple comparisons using the Benjamini-Hochberg false discovery rate procedure, less than 0.05) were visualized by plotting Log2 fold changes in abundance on and off the plateau in ggplot2 v 2.2.1 (Wickham 2011, 2016).

To explore the influence of abiotic factors on community composition, a canonical correspondence analysis (CCA) was

done with the "vegan" R-package on ASVs relative abundances, pooled by genus when this taxonomic level was available. The same analysis was also run only considering ASVs accounting for over 1% of the reads. Significant environmental variables were selected using function ordistep with 1000 permutations, which performs automatic stepwise model building for constrained ordination methods in both directions (forward and backward) based on pseudo-Akaike Information Criterion. No autocorrelation for selected environmental variables was detected using the vif.cca function. Significance of the final model and the different axis was checked using ANOVA (1000 permutations) and the CCA was plotted using ggplot2.

Pigment measurements and CHEMTAX analysis

Pigment extractions for KEOPS 1 and 2 cruises are described in Uitz et al. (2009) and Lasbleiz et al. (2014). In brief, from 1 to 2.2 L, based on particle concentrations, were filtered onto Whatman GF/F filters. For the MOBYDICK cruise, 2.32 L of water was sampled and filtered onto Whatman GF/F filters at each station and depth. Filters were then flash-frozen in liquid nitrogen and stored at -80°C . For all cruises, pigment determination was done using high-performance liquid chromatography (HPLC), following the method of Ras et al. (2008), adapted from Van Heukelem and Thomas (2001). To perform CHEMTAX analysis, HPLC data from all sampling points in the first 50 m were considered.

CHEMTAX v1.95 (Mackey et al. 1996) was used to assess the contribution of seven different taxonomic groups to total chlorophyll a (Chl a): chlorophytes, prasinophytes, cyanobacteria (most likely representative of *Synechococcus*, as *Prochlorococcus* is absent at this latitude), cryptophytes, diatoms, dinoflagellates (with peridinin), and haptophytes (*Phaeocystis* like). This software aims at determining the contribution of different photosynthetic groups to total Chl a biomass based on each group's characteristic accessory pigment to Chl a ratio. Pigment composition characteristic of the different groups was assessed using 11 pigments: chlorophyll $c3$ (Chl $c3$), peridinin (Peri), fucoxanthin (Fuco), prasinoxanthin (Pras), 19'-Hexanoyloxyfucoxanthin (Hex-fuco), zeaxanthin (Zea), alloxanthin (Allo), lutein (Lut), and chlorophyll b (Chl b). An initial matrix of pigment to Chl a ratios for these seven taxonomic groups was build based on previous chemo-taxonomic studies of phytoplankton in the SO (Wright et al. 2010; van Leeuwe et al. 2014) (Supporting Information Table S1).

Samples were first clustered based on their pigment : Chl a ratios to form homogeneous bins using R-software, Hierarchical clustering on principle components (HCPC), implemented in the package FactoMineR (Lê et al. 2008). Then, pigment: Chl a ratios were adjusted for each bin using 60 randomized ratio matrix varying by up to $\pm 35\%$ of the initial ratio matrix to avoid any bias linked to the ratios chosen from the literature. Taxa composition was then inferred for each sample of every cluster based on the average ratios from the six best

runs, associated with the lowest root mean square of the residuals and hence the lowest amount of unexplained pigment. It was then finally ensured that ratios of each characteristic pigment : Chl *a* obtained in the final ratio matrix for each taxonomic group were still in the range accepted in literature sources used in Higgins et al. (2011).

Abundance of autotrophic pico- and nanoplankton

Abundance of pico- and nanoautotrophs was determined by flow cytometry. For all cruises, 4.5 mL of seawater were fixed with glutaraldehyde (1% final concentration). Fixed samples were stored for 30 min at 4°C, flash frozen in liquid nitrogen, and stored at -80°C until analysis (Marie et al. 1999). Counts were performed with BD flow cytometers (FACSCalibur for KEOPS 1, and FACSCanto for KEOPS2 and MOBYDICK cruises) equipped with blue (argon 488 nm) and red (633 nm) lasers. Phytoplankton cells were analyzed according to their natural fluorescence (Chl *a* and phycoerythrin). Approximately 0.75 mL of sample were analyzed at high speed (150 μL min⁻¹) for 5 min as described in Christaki et al. (2014).

Results

Brief description of the physicochemical parameters (MOBYDICK)

During MOBYDICK, phosphate and nitrogen were abundant in the ML at all stations (Table 2). On the plateau (M2), silicic acid concentrations were low (< 2 μmol L⁻¹), especially during the first two visits, but doubled at the last visit after a storm (10 March 2018). M2 was also characterized by the highest ammonium concentrations (0.75–1.1 μmol L⁻¹). Off-plateau, Sta. M1, M3, and M4, presented different physicochemical characteristics for the ML in relation with their location North or South of the polar front, in subantarctic or

Antarctic waters, respectively (Fig. 1c). Silicate concentrations were lower in subantarctic waters at M3 (minimum of 2.3 μmol L⁻¹) than in Antarctic waters at M4 and M1 (from 4.36 to 8.38 μmol L⁻¹). M1 and M4 were located in dynamic water masses near the polar front and were weakly stratified. Consequently, the depth of the ML was shallowest at M1 (27 m) and varied considerably between the two visits at M4 (49 and 87 m). At M2 and M3, ML depth varied between 60 and 80 m and also deepened after the storm (Table 2). Depth of the euphotic layer (Z_e) was always shallower at M2 (45 m) than off the plateau (56–75 m). Lowest temperatures were observed at M4 (4.4°C), south of the plateau, and highest temperatures in subantarctic waters at M3 (5.6°C).

Diversity and community composition of microbial eukaryotes after the diatom bloom

After DADA2 quality filtering, 8328 ASVs were retrieved from a total of 3,366,966 reads in 64 samples. ASVs not assigned to Eukaryotes or assigned to Metazoa were removed leaving a total of 8164 ASVs and 3,356,832 reads. After removing singletons, 5831 ASVs and 3,355,898 reads were kept for further analysis. One sample with less than 5000 reads was excluded from the analysis (M2-3, 60 m, < 20 μm).

The number of observed ASVs per sample ranged from 116 (M2-1, 125 m, < 20 μm) to 648 (M4-2, 125 m, < 20 μm). The mean observed richness across all stations and depths was significantly higher in the small than in the large size fraction. Richness was not different on and off the plateau for each size fraction. Within the small size fraction, richness differed according to depth and was overall higher at 125 and 300 m than at 10 m (Fig. 2). Highest richness was observed off the plateau at M4 (125 m) with over 600 different ASVs sequenced at each visit and lowest richness on the plateau at M2 (125 m) with only 116 ASVs (Fig. 2). No differences in evenness

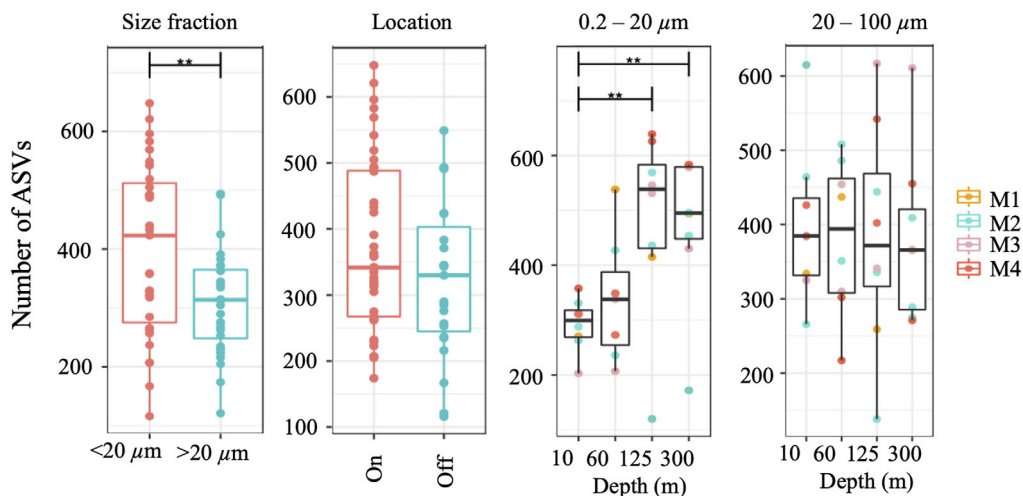


Fig. 2. Richness for the entire data set according to different size fractions and locations on or off the plateau, and for each depth of the different size fractions. Pairwise significant differences (Tukey HSD, *p* < 0.05) are indicated.

between the two size fractions could be identified, although it was overall higher off the plateau. Within the small size fraction, evenness was significantly higher at 125 m than at 10 m (Supporting Information Fig. S1). Although all taxonomic orders were found in the two size fractions, small and large size fraction community composition differed significantly at all depths (PERMANOVA, $p < 0.001$).

Surface samples of the $< 20 \mu\text{m}$ size fraction were dominated either by parasitic Syndiniales (55–78% at M2-1, M2-2, M3-1) or Haptophytes (*Phaeocystis*) (10–46%; Fig. 3). Small diatoms (in the $< 20 \mu\text{m}$ fraction) were more abundant at Sta. M1 and M4 off-plateau, where they accounted for 21% and up to 30% of the reads, respectively, but represented less than 10% of the reads at M2 and M3. Other phytoplankton, such as

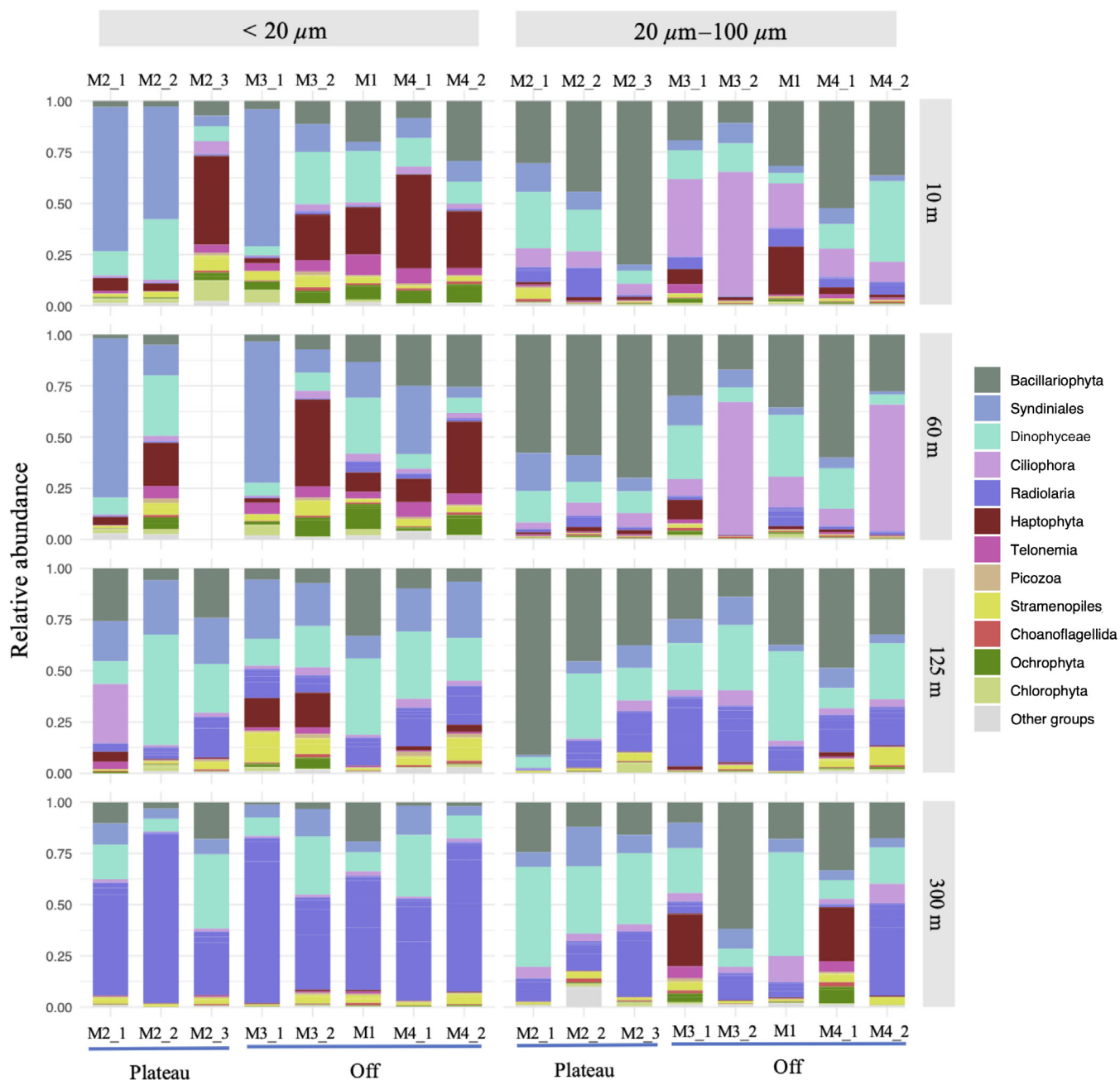


Fig. 3. Relative abundance of high-level taxonomic groups at each station and depth for both size fractions. Bacillariophyta have been distinguished from other Ochrophyta and Syndiniales from core dinoflagellates Dinophyceae (Dinoflagellata) to highlight these two taxonomic groups. “Other groups” include rare taxonomic groups representing together less than 0.1% of the reads. Numbers close to each station refer to the order of visits when stations were visited several times (see Table 2).

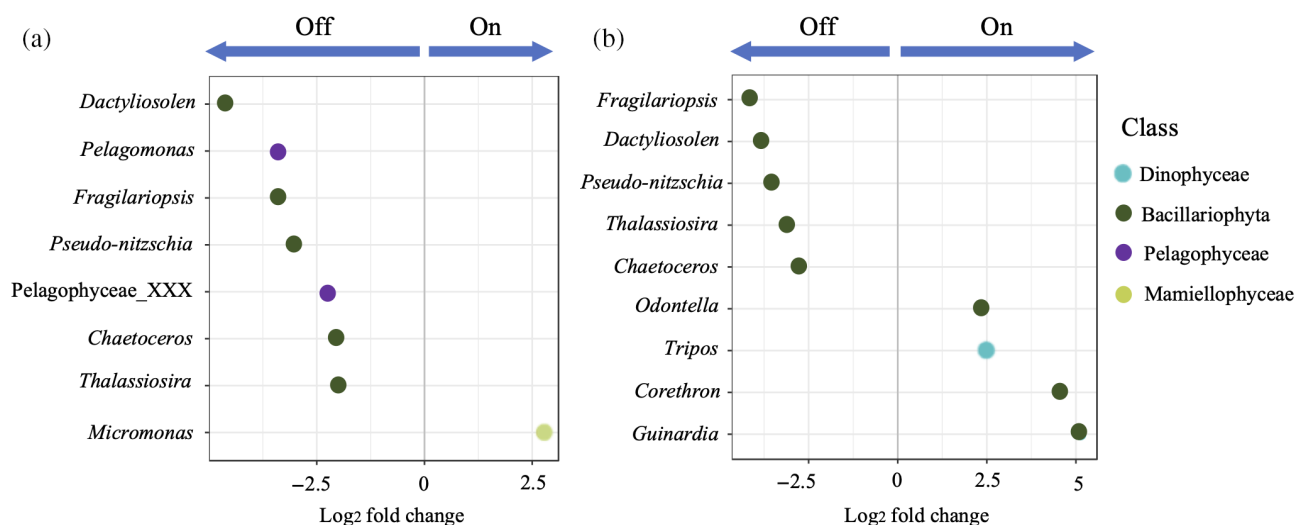


Fig. 4. Phytoplankton genera presenting differential read abundances between surface samples collected on and off plateau after Deseq2 analysis ($p < 0.05$) for small (a) and large size-fractions (b). Only most abundant genera (> 0.1% of total reads and base mean after Deseq2 normalization superior to 100 reads) are represented. A negative log2 fold change indicates genera that are relatively more abundant off the plateau, while a positive log2 fold change indicates genera relatively more abundant on the plateau.

Ochrophyta (Pelagophyceae) and Chlorophyta (Mamiellophyceae and Prasinococcales), were also present in the small size fraction, but accounted for a low proportion of reads at each station (less than 10%). Picograzers such as Telonemia and Stramenopiles (MAST and MOCH; Fig. 3) were also consistently observed at all surface stations in reduced proportions (less than 10% of the reads). An increase of Dinophyceae and Radiolaria was observed at 125 and 300 m depth. Syndiniales, Stramenopiles, and Haptophytes were also present (Fig. 3). At 300 m, the small size fraction was largely dominated by Radiolaria (31–83%), and Dinophyceae (7–36%).

Surface samples (10 and 60 m) of the large size fraction were dominated by Bacillariophyta (up to 80% at M2-3) or Ciliophora (up to 65% at M3-3, 60 m; Fig. 3). Diatoms were still present (14–91%) deeper at 125 m and contributed up to 91% of the reads at Sta. M2-1 with a marked contribution of *Odontella* and *Eucampia* (Supporting Information Fig. S2). The relative abundance of Dinophyceae and Radiolaria increased at this depth as in the small size fraction. Finally, the large size fraction consisted mainly of an assemblage of dinoflagellates, Radiolaria, Syndiniales, and Bacillariophyta at 300 m depth. Small phytoplanktonic Haptophyta (*Phaeocystis*) represented up to 25% of the reads at 300 m at M3-1 and M4-1 (Fig. 3, Supporting Information Fig. S2) when they were almost absent in this size-fraction in the upper layers.

When looking only at autotrophic taxa of the small size fraction in surface samples (10 and 60 m), phytoplankton communities were different on and off the plateau (PERMANOVA; $p = 0.04$). *Phaeocystis* was present in all surface samples, but a few common autotrophic taxa were enhanced in these distinct regions (DESeq2 analysis; Fig. 4a). *Pelagomonas* and unidentified Pelagophyceae were more

abundant off the plateau in contrast with the prasinophyte *Micromonas* (Mamiellophyceae) that was more abundant on the plateau. Diatoms belonging to the genera *Fragilariopsis*, *Pseudo-nitzschia*, *Dactyliosolen*, *Thalassiosira*, and *Chaetoceros* were enriched off the plateau (Fig. 4a). *Fragilariopsis*, *Pseudo-nitzschia*, *Dactyliosolen*, *Thalassiosira*, and *Chaetoceros* were also enriched off the plateau in the large size fraction, whereas reads of the diatoms *Corethron* and *Guinardia* were more abundant on the plateau (Fig. 4b).

Relation between environmental variables and community composition in late summer

CA analyses of surface euphotic layer samples and main environmental variables emphasized a clear distinction between on and off-plateau communities (Fig. 5). *Phaeocystis*, which was abundant in surface waters of all stations, appeared in the middle of the CCA, as it was not related to any particular environmental parameter. Among the environmental variables tested, ammonium, phosphate, temperature, and silicic acid were significant predictors of community composition within the small size fraction when considering all ASVs and/or only the most common ASVs (automatic stepwise model building analysis, $p < 0.01$). None of these variables showed significant auto-correlation and they explained 45.8% of the variance of the entire community composition within the small size fraction (CCA1 = 15.1%; CCA2 = 12.4%; CCA3 = 10.3%; CCA4 = 8.0%). When plotting on the CCA small phytoplankton taxa that were differentially abundant on and off the plateau (cf. Fig. 4a), plateau station M2 was characterized by higher ammonium concentrations along with higher abundances of the prasinophyte *Micromonas* (Mamiellaceae family). Diatoms such as *Fragilariopsis*, *Thalassiosira*, and *Pseudo-nitzschia* were associated off the plateau

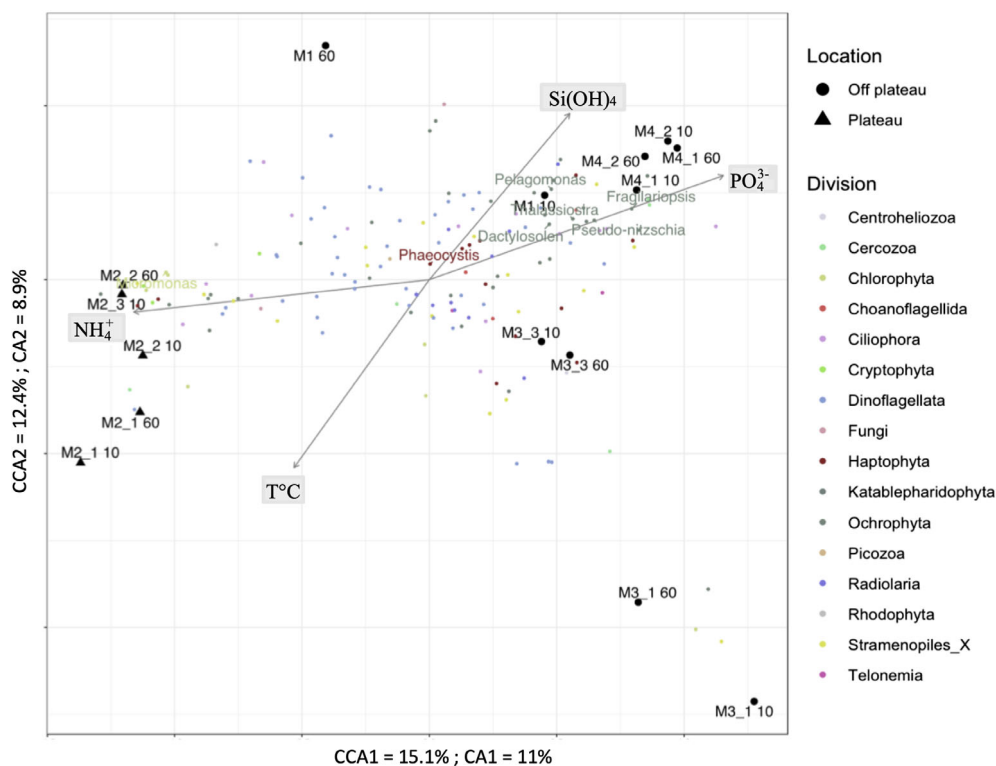


Fig. 5. Ordination diagram (CCA) of small protist taxonomic groups at surface (all ASVs) and significant abiotic variables (ammonium [NH₄⁺], phosphate [PO₄³⁻], silicic acid [Si(OH)₄], and temperature [T, °C]). Black marks are representative of the community composition of each sample, labeled by station and depth. The different genera (or ASVs when this taxonomic level was not available) are represented by dots colored by division. Only the genera/ASVs representing more than 1% of total reads were plotted, to not overload the chart. Only phytoplankton genera considered as differentially abundant between stations on and off plateau according to DESeq2 were labeled. *Phaeocystis* position in the middle of the CCA plot indicated its presence at all stations.

with M1 and M4 as well as the highest concentrations of silicic acid and phosphate (Fig. 5).

Seasonal changes in phytoplankton assemblages

CHEMTAX analyses highlighted that phytoplankton communities were contrasted on and off the plateau at the onset and the decline of the Kerguelen bloom (KEOPS 1 and 2, respectively). In late summer (MOBYDICK), small phytoplankton—prymnesiophytes particularly—was important over the entire area (Fig. 6). On the plateau, contribution of the different phytoplankton groups varied markedly over seasons (Fig. 6a,c). Diatoms dominated phytoplankton blooms in spring and summer (KEOPS 2 and 1), while small flagellates represented higher proportions of the phytoplankton community in late summer (MOBYDICK, Fig. 6c). During spring and summer blooms (KEOPS 2 and 1), Chl *a* was sixfold higher on the plateau than off-plateau reference stations (1.21 ± 0.26 μg L⁻¹ and 0.19 ± 0.05 μg L⁻¹, respectively) and diatom pigments represented over 90% of Chl *a* (Fig. 6a,c). Concomitantly, only prymnesiophytes remained at low background levels within small phytoplankton taxa. In late summer (MOBYDICK), Chl *a* on the plateau dropped to values similar to the ones found off the plateau

(0.3 ± 0.02 μg L⁻¹ at M2-1 and M2-2; Fig. 6a,b). These low Chl *a* concentrations were mainly due to a strong (22-fold) decrease of diatoms' contribution to Chl *a* (from up to 1.8 μg L⁻¹ in November to 0.08 μg L⁻¹ end of February). As a consequence of the diatom decline, small nonsilicified phytoplankton's contribution strongly increased on the plateau after the bloom, with prymnesiophytes and prasinophytes accounting for 53–58% of Chl *a* (Fig. 6a,c). The contribution of prasinophytes notably increased from 5.7% to 16.6% between the first and last visit at M2 during late summer (MOBYDICK). They also contributed to 8.9% to Chl *a* biomass at the very early stage of the bloom (KEOPS2, first visit). Total abundances of small phytoplanktonic cells after the bloom (3200–8300 cells mL⁻¹) were also much higher after the bloom than during the bloom (700–2000 cells L⁻¹).

Off the plateau, Chl *a* was low during the three cruises (0.20 ± 0.05 μg L⁻¹; Fig. 6b). Prymnesiophytes, followed by diatoms, were the most represented groups in pigment data, with average relative contribution to Chl *a* of 51.6% and 39.3%, respectively. Pigments characteristic of small nonsilicified phytoplankton dominated at all off-plateau reference stations (Fig. 6b), with the exception of Sta. C11-1

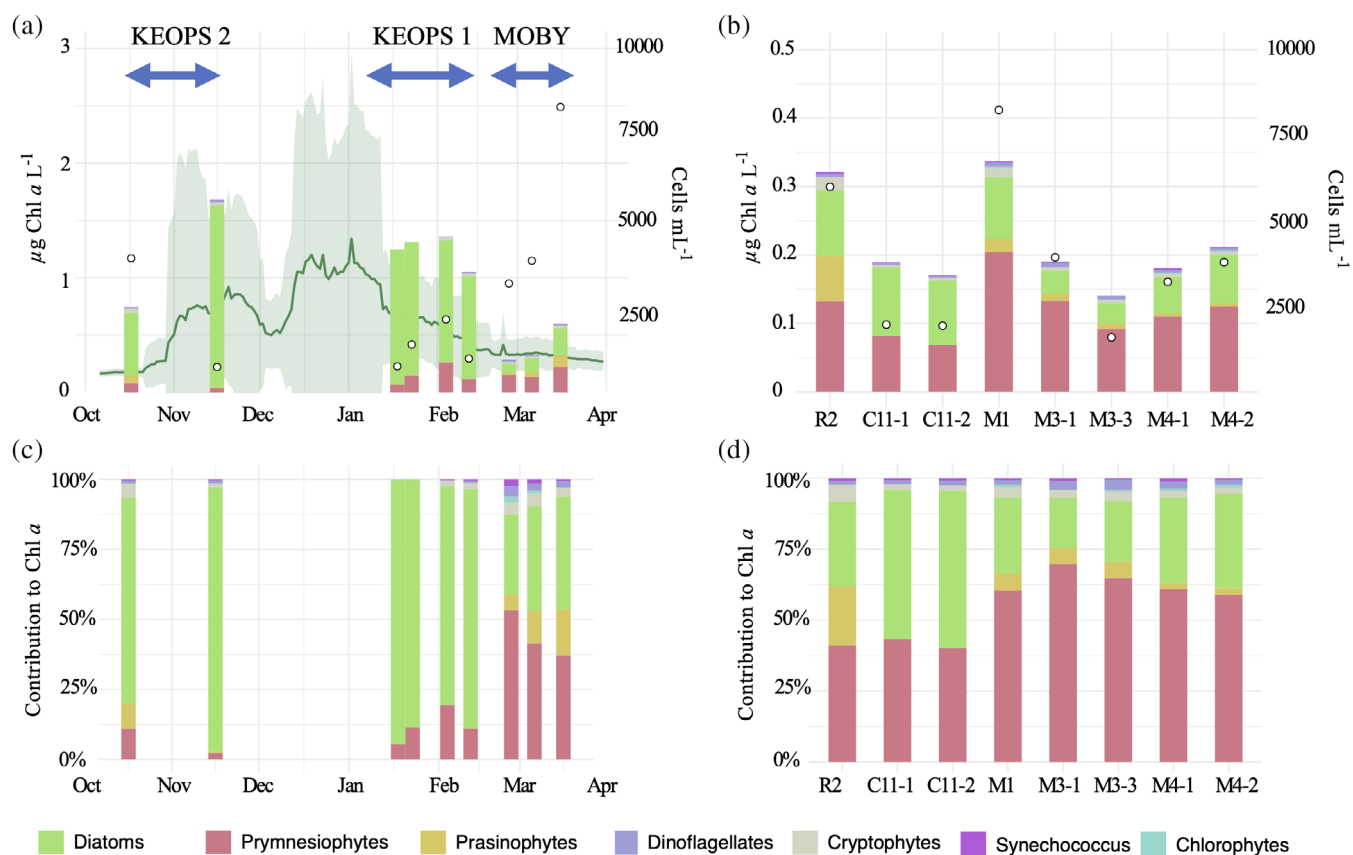


Fig. 6. Average estimated contribution of CHEMTAX groups to Chl *a* biomass ($\mu\text{g L}^{-1}$) and abundance of small phytoplankton measured by flow cytometry (open circles, cells mL^{-1}) in the 50 upper meters for plateau station (a) and HNLC reference stations (b) sampled during KEOPS 1-2 and MOBYDICK. Note different scales on Y-axis. In figure (a), average climatological mean (green line) and standard deviation (green area) estimated from satellite data on the plateau are indicated. Relative contribution of the different groups to total Chl *a* for plateau station (c) and HNLC reference stations (d).

(KEOPS1 HNLC reference station) where diatom pigments accounted for 52.1% of Chl *a*. Prymnesiophytes were the most important group and represented up to 70% of Chl *a* (M3-1; Fig. 6d). Other groups were minor contributors to Chl *a*, with the exception of prasinophytes at R2 (20.7%). As a consequence of these contrasted phytoplankton communities on and off the plateau, Chl *a* was significantly correlated with the abundance of small phytoplankton only off the plateau ($R^2 = 0.89$; $p < 0.0001$; Supporting Information Fig. S3).

Discussion

The MOBYDICK cruise provided first insights into the phytoplankton community around Kerguelen after the summer bloom. Data from this study highlight the dominance of small-sized phytoplankton off the plateau (HNLC) throughout the year and document for the first time their importance in phytoplankton communities in surface waters on the Kerguelen plateau. The intense diatom blooms on the Kerguelen plateau are thus followed by an increase of small phytoplankton in terms of absolute and relative contribution to

Chl *a* (Fig. 6a,b), displaying a seasonal community succession observed in other regions of the SO (e.g., Moline et al. 1996; Fiala et al. 1998; Wright et al. 2010). This study has further highlighted that small phytoplankton communities differed on and off the plateau in relation with contrasting nutrients concentrations (ammonium and silicic acid) after the bloom (Fig. 7).

Diversity of pico- and nanophytoplankton and their response to environmental variables

Both CHEMTAX and sequencing analyses suggested that Prymnesiophytes, dominated by *Phaeocystis antarctica*, were the most abundant phytoplankton group in late summer. This phytoplanktonic group represented up to 53% and 70% of the Chl *a* on and off the plateau, respectively (Fig. 6c,d). Contrasted environmental conditions on and off the plateau did not seem to affect their distribution (Fig. 5). The ability of *P. antarctica* to thrive in HNLC waters has been explained by its large phenotypic plasticity, being able to reduce its cell volume and adapt its photo-physiology under Fe-limitation (Alderikamp et al. 2012; Koch et al. 2019). Iron replete conditions are known to trigger

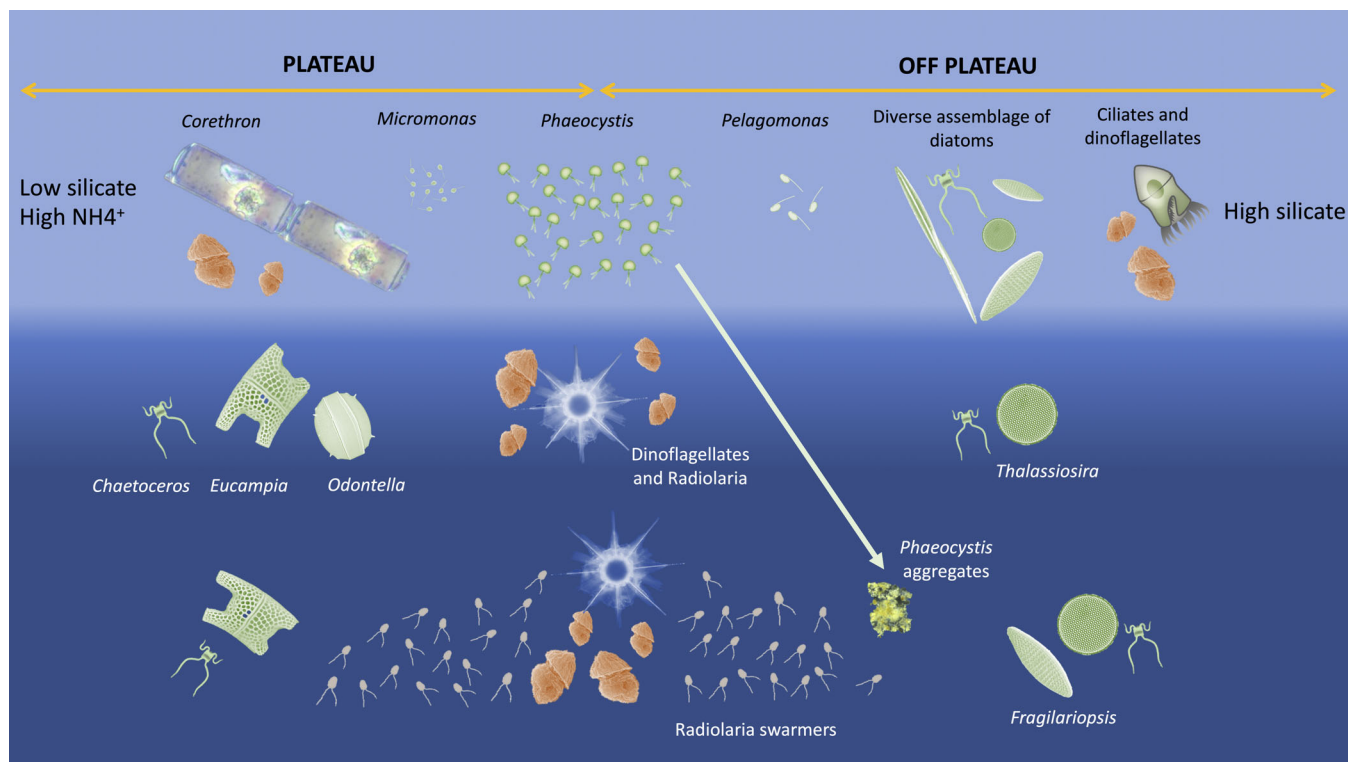


Fig. 7. Schematic graph of the dominating microbial eukaryotes after the bloom based on 18s rRNA metabarcoding. At 10 and 60 m (light blue on the figure), *Phaeocystis* was abundant on and off the plateau. On the plateau, where silicate concentrations were low and ammonium concentrations high, phytoplankton community was characterized by the dominance of large and lightly silicified diatom belonging to the genus *Corethron* and the presence of prasinophyte *Micromonas* in the small size-fraction (Fig. 4a). Off the plateau, silicate concentrations were not limiting and promoted a diverse assemblage of diatoms (*Fragilariopsis*, *Thalassiosira*, *Pseudo-nitzschia*, *Chaetoceros*) in both small and large-size fractions (Fig. 4a). Small and large heterotrophic dinoflagellates were well represented everywhere and ciliates were particularly abundant in some samples of the large size fraction off the plateau (Fig. 3). Below the ML (125 m), the relative abundance of heterotrophic dinoflagellates and Radiolaria increased. At 300 m, the small size fraction was largely dominated at all stations by Radiolaria, probably as swimmers stages (Fig. 3). Large, heavily silicified diatoms (*Eucampia* and *Odontella* on the plateau; *Thalassiosira* and *Fragilariopsis* off the plateau) characterized phytoplankton community (Supporting Information Fig. S2). *Chaetoceros* was also present, mostly in the small size fraction on the plateau and at M1. *Phaeocystis*, probably forming aggregates, was detected in large proportions only at 300 m off the plateau (Fig. 3).

Phaeocystis colony formation (Garcia et al. 2009; Bender et al. 2018). Colony formation and size increase could in turn serve as defense mechanisms against small grazers such as copepods and ciliates (Schoemann et al. 2005; Tang et al. 2008). As a consequence, previous studies conducted in the SO observed that *Phaeocystis* population was mostly composed of single cells before and after the phytoplankton bloom. In spring, optimal light and iron concentrations lead to the formation of colonies (Smith et al. 2003). At the onset of the spring bloom (KEOPS2, November), when surface dissolved iron concentration was at its highest (Blain et al. 2007; Bowie et al. 2015), *Phaeocystis* was observed on and off the plateau in small colonies (Georges et al. 2014). This feature probably made them more resistant to grazing by protists than free cells like prasinophytes, as shown by the strong decrease of prasinophytes between the first two visits on the plateau during KEOPS2 (Fig. 6a,c). In late summer (MOBYDICK), *Phaeocystis* was only observed as small flagellated single cells (approximately 3 μm, electron microscopy

observations, Supporting Information Fig. S4) on and off the plateau, in agreement with a potential iron limitation after the phytoplankton bloom (Smith et al. 2003).

While sequencing data indicated that *P. antarctica* was relatively abundant at all stations after the bloom, the structure of the other small phytoplanktonic groups featured marked differences on and off the plateau. Free *Phaeocystis* cells, *Micromonas*, and *Pelagomonas* are mostly grazed by ciliates, whose prey generally falls within the nanophytoplankton size class (Hansen et al. 1994). During MOBYDICK, ciliate communities showed similar structures and abundances on and off the plateau (Christaki, pers comm), suggesting that the observed spatial variability of small phytoplankton was most likely related to the availability of specific nutrients. High NH₄⁺ concentrations on the plateau (0.75–1.1 μmol L⁻¹) coincided during MOBYDICK with an increase in relative abundance of *Micromonas* (Figs. 5, 7). Increased ammonium concentrations on the plateau have previously been observed during the bloom decay (KEOPS1),

and were attributed to high heterotrophic activity (Mosseri et al. 2008). Ammonium is less energetically costly to assimilate than nitrate and is as such the preferred dissolved nitrogen source for most microalgae (McCarthy 1981; Raven et al. 1992), especially for prasinophytes (Litchman et al. 2007). They are thus able to grow more efficiently than other phytoplanktonic groups when ammonium concentrations are high. Slightly warmer temperatures on the plateau than off the plateau might also represent an advantage for prasinophytes. In the SO, other CHEMTAX studies have reported prasinophytes mostly north of 51°S (Wright et al. 1996), particularly in the Sub Tropical Front, where they could represent up to 10% of Chl *a* biomass (Iida and Odate 2014). In our study area, prasinophytes were mostly found close to the polar front during the onset (R-2, KEOPS2, Georges et al. 2014) and after the bloom (Sta. M2 and M3, MOBYDICK, Fig. 6d). When the Arctic *Micromonas* thrive in a cold and ice-covered ocean (Lovejoy et al. 2007), its close phylogenetic counterpart inhabiting the SO seems to be favored by warmer waters, suggesting differentiation into two distinct ecotypes.

Pelagophytes were enriched in Antarctic waters off the plateau (Figs. 4a, 7). During the LOHAFEX artificial iron experiment, pelagophytes were common in iron limited waters, but their relative abundance in sequencing datasets decreased after iron fertilization, whereas *Micromonas* became more abundant (Thiele et al. 2014). Experimental studies also demonstrated that *Pelagomonas* had higher affinities for dissolved inorganic iron than another prasinophyte *Prasinomonas* (Timmermans et al. 2005). If the same is true for other prasinophytes, *Pelagomonas* could thus be more competitive when iron is limiting, whereas *Micromonas* could be characterized as an opportunistic species, able to rapidly grow on ammonium.

Balance between small nonsilicified phytoplankton and diatoms (small and large)

At the bloom onset, when silicate and iron were not limiting, diatoms were able to build up biomass more efficiently than small nonsilicified phytoplankton whose abundance decreased (Fig. 6a; Supporting Information Table S2). Diatom grazers have relatively long generation times, leaving time for diatoms to proliferate until predation pressure control their population (Smetacek et al. 2004). Small nonsilicified phytoplankton are more rapidly controlled by predators, composed of fast growing microzooplankton such as ciliates and dinoflagellates (Coale et al. 1996; Landry et al. 2002, 2011; Smetacek et al. 2004). During the decline and after the bloom on the plateau, the scarcity of silicate ($18.7 \mu\text{mol L}^{-1}$ in October in KEOPS2 to less than $2 \mu\text{mol L}^{-1}$ during MOBYDICK; Supporting Information Table S2) and iron likely explains the collapse of diatom populations (Mosseri et al. 2008).

During MOBYDICK, diatom communities differed between on and off-plateau stations. According to sequencing data of the $< 20 \mu\text{m}$ fraction, a diverse assemblage of small diatoms, such as *Fragilariopsis*, *Pseudo-nitzschia*, *Thalassiosira*, and

Chaetoceros, was enriched in Antarctic waters off the plateau (M4 and M1), probably related to higher silicate concentrations (Figs. 5, 7). The same diatom genera were also enriched in the large size fraction (Fig. 4b) and microscopic observations confirmed that their size range overlapped the two size fractions. In contrast, a few large diatoms were enriched on the plateau (Fig. 4b), where the lowest concentrations in $\text{Si}(\text{OH})_4$ were observed ($< 2 \mu\text{mol L}^{-1}$ during the first two visits). Silicate requirements as well as Si uptake kinetics can vary from one species to the other. However, Hoffmann et al. (2008) suggested that silicate depletion may limit small diatoms sooner than large diatoms since the amount of silica needed relative to the volume of the cell is higher for small diatoms. In contrast, small diatoms were likely advantaged off the plateau (Sta. M1 and M4), where silicic acid concentration was higher. When silicate concentrations remain sufficient to build the frustules, cell size reduction is a morphological adaptation of diatoms to low iron concentrations, as an increased surface to volume ratio could facilitate iron uptake (Leynaert et al. 2004; Marchetti and Cassar 2009). In addition to their small size, most diatom genera that were enriched off the plateau in our study possess particular physiological adaptations to cope with low iron concentrations. The pennate diatoms *Pseudo-nitzschia* and *Fragilariopsis* use the iron-concentrating protein Ferritin, which allows them to store more iron than centric diatoms (Marchetti et al. 2009). The centric diatom *Thalassiosira* is adapted to low iron concentrations by possessing a modified photosynthetic apparatus, with electron-transport proteins modified to use copper instead of iron (Peers and Price 2006). It is also supposed to have an efficient iron vacuolar storage mechanism (Nuester et al. 2012). Sta. M3 was located in subantarctic waters and differed from the two other Antarctic water influenced off-plateau stations (M1, M4). M3 presented low silicate concentrations and lowest Chl *a* (Table 2). M3 showed the lowest proportion of diatom pigments (25% of Chl *a*) and number of reads in both small and large size fractions suggesting silicate and iron colimitation which disadvantaged growth of all diatoms.

Microbial eukaryotes below the ML and potential implications

Surface phytoplankton communities dominated by small cells, as observed during MOBYDICK cruise, are expected to sustain an active microbial loop. This implies little direct export of small phytoplankton production to the deep ocean, most of it being rapidly remineralized (Michaels and Silver 1988; Martin et al. 2013). Molecular analysis showed that the relative contribution of *Phaeocystis* strongly decreased below the ML in the small size fraction. The relative contribution of diatoms to the total amount of reads remained unchanged at 125 m and decreased at 300 m in this size fraction (Fig. 3). In the large size fraction, diatoms still accounted for over 25% of total number of reads in some off-plateau deep samples (M3-2 and M4-1, 300 m). *Thalassiosira* and

Fragilariopsis, which were recorded in both small and large size fractions at the surface in off-plateau waters, were found only in the large size fraction at 300 m (Supporting Information Figs. S2, S5). Lightly silicified *Corethron* dominated at the surface on the plateau during MOBYDICK (Supporting Information Fig. S2) while *Chaetoceros*, *Eucampia*, and *Odontella* were the main diatoms detected at 125 m depth (M2-3; Supporting Information Figs. S2, S5b). This suggests that small diatoms are not as efficiently exported as their larger counterparts. It also supports the hypothesis that the higher carbon export efficiency recorded off the plateau in summer (up to 58% of net primary production during KEOPS1) could be due to direct export of large fast sinking heavy silicified diatoms, assumed to be grazing-resistant (Laurenceau-Cornec et al. 2015).

Interestingly, *Phaeocystis* was found in relatively high proportions off the plateau (M3 and M4) at 300 m in the large size-fraction (Fig. 3). Although vertical carbon flux attenuation is higher for *Phaeocystis* than for diatoms (Reigstad and Wassmann 2007), *Phaeocystis* blooms have been shown to greatly contribute to carbon export in the Ross Sea (DiTullio et al. 2000). In our study, only single cells of *Phaeocystis* were observed in surface samples (Supporting Information Fig. S5). Considering the essential role of iron in colony formation, we consider unlikely that the presence of a relatively abundant number of reads at 300 m could result from direct sinking of colonies forms in previous weeks. This suggests that single cells of *Phaeocystis* could be exported directly through aggregation and/or indirectly through grazing (Reigstad and Wassmann 2007; Richardson and Jackson 2007; Richardson 2018). Grazers, such as dinoflagellates and Radiolaria, were the most common organisms in both size-fractions in the deeper samples (Figs. 3, 7). These predators are able to feed on a wide variety of size classes, from small cells to chain-forming diatoms (Swanberg and Caron 1991; Sherr and Sherr 2007). Previous studies have reported their high abundance at the bottom of the ML where they may feed on diatoms and other sinking cells and particles (Christaki et al. 2008, 2015; Gomi et al. 2010). The small fraction of deeper samples was largely dominated on and off-plateau by Radiolaria swimmers belonging to Chaunacanthidae family (cluster 4; Supporting Information Fig. S5b; Fig. 7). This group can form large cysts that can sink from the surface to deep waters where they release thousands of swimmers (< 5 μm) after the bloom. They may then use surface-produced organic carbon as a nutritional source while ascending through the water column (Martin et al. 2010; Decelle et al. 2013).

Concluding, global-change models project more stratified waters over the plateau of Kerguelen, increasing silicate and iron limitations (Freeman et al. 2018). Iron and silicate depleted waters are known to favor small phytoplankton communities over large ones—as observed during MOBYDICK—and eventually reduce carbon export due to promotion of microbially dominated food webs and greater remineralization (Bowie et al. 2011; Ebersbach et al. 2011; Martin et al. 2013).

Our study has shown contrasting small phytoplankton community structures relative to available nutrients on and off the Kerguelen plateau, and also underlined the capacity of *Phaeocystis* to thrive all over the studied region. In addition, this study has also highlighted that the possible contribution of *Phaeocystis* to carbon export in low productivity conditions deserves to be further studied.

References

- Agawin, N. S. R., C. M. Duarte, and S. Agustí. 2000. Nutrient and temperature control of the contribution of picoplankton to phytoplankton biomass and production. *Limnol. Oceanogr.* **45**: 591–600. doi:10.4319/lo.2000.45.3.0591
- Alderkamp, A.-C., G. Kulk, A. G. J. Buma, R. J. W. Visser, G. L. Van Dijken, M. M. Mills, and K. R. Arrigo. 2012. The effect of iron limitation on the photophysiology of *Phaeocystis antarctica* (Prymnesiophyceae) and *Fragilariopsis cylindrus* (Bacillariophyceae) under dynamic irradiance. *J. Phycol.* **48**: 45–59. doi:10.1111/j.1529-8817.2011.01098.x
- Aminot, A., and R. K erouel. 2007. Dosage automatique des nutriments dans les eaux marines: M ethodes en flux continu. Editions Quae.
- Andersen, K. S., R. H. Kirkegaard, S. M. Karst, and M. Albertsen. 2018. ampvis2: An R package to analyse and visualise 16S rRNA amplicon data. bioRxiv 299537. doi:10.1101/299537
- Armand, L. K., V. Cornet-Barthaux, J. Mosseri, and B. Qu eguiner. 2008. Late summer diatom biomass and community structure on and around the naturally iron-fertilised Kerguelen Plateau in the Southern Ocean. *Deep-Sea Res. Part II Top. Stud. Oceanogr.* **55**: 653–676. doi:10.1016/j.dsr2.2007.12.031
- Bender, S. J., and others. 2018. Colony formation in *Phaeocystis antarctica*: Connecting molecular mechanisms with iron biogeochemistry. *Biogeosciences* **15**: 4923–4942. doi:10.5194/bg-15-4923-2018
- Blain, S., and others. 2007. Effect of natural iron fertilization on carbon sequestration in the Southern Ocean. *Nature* **446**: 1070–1074. doi:10.1038/nature05700
- Bower, S. M., R. B. Carnegie, B. Goh, S. R. Jones, G. J. Lowe, and M. W. Mak. 2004. Preferential PCR amplification of parasitic protistan small subunit rDNA from metazoan tissues. *J. Eukaryot. Microbiol.* **51**: 325–332. doi:10.1111/j.1550-7408.2004.tb00574.x
- Bowie, A. R., T. W. Trull, and F. Dehairs. 2011. Estimating the sensitivity of the subantarctic zone to environmental change: The SAZ-Sense project. *Deep-Sea Res. Part II Top. Stud. Oceanogr.* **58**: 2051–2058. doi:10.1016/j.dsr2.2011.05.034
- Bowie, A. R., P. van der Merwe, F. Qu erou e, and others. 2015. Iron budgets for three distinct biogeochemical sites around the Kerguelen Archipelago (Southern Ocean) during the

- natural fertilisation study, KEOPS-2. *Biogeosciences* **12**: 4421–4445. doi:[10.5194/bg-12-4421-2015](https://doi.org/10.5194/bg-12-4421-2015)
- Callahan, B. J., P. J. McMurdie, M. J. Rosen, A. W. Han, A. J. A. Johnson, and S. P. Holmes. 2016. DADA2: High-resolution sample inference from Illumina amplicon data. *Nat. Methods* **13**: 581–583. doi:[10.1038/nmeth.3869](https://doi.org/10.1038/nmeth.3869)
- Caporaso, J. G., and others. 2010. QIIME allows analysis of high-throughput community sequencing data. *Nat. Methods* **7**: 335–336. doi:[10.1038/nmeth.f.303](https://doi.org/10.1038/nmeth.f.303)
- Cavagna, A. J., and others. 2015. Production regime and associated N cycling in the vicinity of Kerguelen Island, Southern Ocean. *Biogeosciences* **12**: 6515–6528. doi:[10.5194/bg-12-6515-2015](https://doi.org/10.5194/bg-12-6515-2015)
- Chisholm, S. W. 1992. Phytoplankton size, p. 213–237. In P. G. Falkowski, A. D. Woodhead, and K. Vivirito [eds.], *Primary productivity and biogeochemical cycles in the sea*. Springer.
- Christaki, U., I. Obernosterer, F. Van Wambeke, M. Veldhuis, N. Garcia, and P. Catala. 2008. Microbial food web structure in a naturally iron-fertilized area in the Southern Ocean (Kerguelen Plateau). *Deep Sea Research Part II: Topical Studies in Oceanography*. **55**: 706–719. doi:[10.1016/j.dsr2.2007.12.009](https://doi.org/10.1016/j.dsr2.2007.12.009)
- Christaki, U., and others. 2014. Microbial food web dynamics during spring phytoplankton blooms in the naturally iron-fertilized Kerguelen area (Southern Ocean). *Biogeosciences*. **11**: 6739–6753. doi:[10.5194/bg-11-6739-2014](https://doi.org/10.5194/bg-11-6739-2014)
- Christaki, U., C. Georges, S. Genitsaris, and S. Monchy. 2015. Microzooplankton community associated with phytoplankton blooms in the naturally iron-fertilized Kerguelen area (Southern Ocean). *FEMS Microbiol. Ecol.* **91**: 1–15. doi:[10.1093/femsec/fiv068](https://doi.org/10.1093/femsec/fiv068)
- Clarke, L. J., and B. E. Deagle. 2018. Eukaryote plankton assemblages in the southern Kerguelen Axis region: Ecological drivers differ between size fractions. *Deep-Sea Res. Part II Top. Stud. Oceanogr.* **174**: 1–12. doi:[10.1016/j.dsr2.2018.12.003](https://doi.org/10.1016/j.dsr2.2018.12.003)
- Coale, K. H., and others. 1996. A massive phytoplankton bloom induced by an ecosystem-scale iron fertilization experiment in the equatorial Pacific Ocean. *Nature* **383**: 495–501. doi:[10.1038/383495a0](https://doi.org/10.1038/383495a0)
- de Baar, H. J. W., J. T. M. de Jong, D. C. E. Bakker, B. M. Löscher, C. Veth, U. Bathmann, and V. Smetacek. 1995. Importance of iron for plankton blooms and carbon dioxide drawdown in the Southern Ocean. *Nature* **373**: 412–415. doi:[10.1038/373412a0](https://doi.org/10.1038/373412a0)
- Decelle, J., and others. 2013. Diversity, ecology and biogeochemistry of cyst-forming acantharia (radiolaria) in the oceans. *PLoS One* **8**: e53598. doi:[10.1371/journal.pone.0053598](https://doi.org/10.1371/journal.pone.0053598)
- del Campo, J., and others. 2018. EukRef: Phylogenetic curation of ribosomal RNA to enhance understanding of eukaryotic diversity and distribution. *PLOS Biol.* **16**: e2005849. doi:[10.1371/journal.pbio.2005849](https://doi.org/10.1371/journal.pbio.2005849)
- Detmer, A. E., and U. V. Bathmann. 1997. Distribution patterns of autotrophic pico- and nanoplankton and their relative contribution to algal biomass during spring in the Atlantic sector of the Southern Ocean. *Deep-Sea Res. Part II Top. Stud. Oceanogr.* **44**: 299–320. doi:[10.1016/S0967-0645\(96\)00068-9](https://doi.org/10.1016/S0967-0645(96)00068-9)
- Díez, B., C. Pedrós-Alió, and R. Massana. 2001. Study of genetic diversity of eukaryotic picoplankton in different oceanic regions by small-subunit rRNA gene cloning and sequencing. *Appl. Environ. Microbiol.* **67**: 2932–2941. doi:[10.1128/AEM.67.7.2932-2941.2001](https://doi.org/10.1128/AEM.67.7.2932-2941.2001)
- Díez, B., R. Massana, M. Estrada, and C. Pedrós-Alió. 2004. Distribution of eukaryotic picoplankton assemblages across hydrographic fronts in the Southern Ocean, studied by denaturing gradient gel electrophoresis. *Limnol. Oceanogr.* **49**: 1022–1034. doi:[10.4319/lo.2004.49.4.1022](https://doi.org/10.4319/lo.2004.49.4.1022)
- DiTullio, G. R., and others. 2000. Rapid and early export of *Phaeocystis antarctica* blooms in the Ross Sea, Antarctica. *Nature* **404**: 595–598. doi:[10.1038/35007061](https://doi.org/10.1038/35007061)
- Ebersbach, F., T. W. Trull, D. M. Davies, and S. G. Bray. 2011. Controls on mesopelagic particle fluxes in the Sub-Antarctic and Polar Frontal Zones in the Southern Ocean south of Australia in summer—perspectives from free-drifting sediment traps. *Deep-Sea Res. Part II Top. Stud. Oceanogr.* **58**: 2260–2276.
- Edgar, R. C. 2013. UPARSE: Highly accurate OTU sequences from microbial amplicon reads. *Nat. Methods* **10**: 996–998.
- Fiala, M., E. E. Kocczynska, C. Jeandel, L. Oriol, and G. Vétion. 1998. Seasonal and interannual variability of size-fractionated phytoplankton biomass and community structure at station Kerfix, off the Kerguelen Islands, Antarctica. *J. Plankton Res.* **20**: 1341–1356. doi:[10.1093/plankt/20.7.1341](https://doi.org/10.1093/plankt/20.7.1341)
- Freeman, N. M., N. S. Lovenduski, D. R. Munro, K. M. Krumhardt, K. Lindsay, M. C. Long, and M. MacLennan. 2018. The variable and changing Southern Ocean Silicate Front: Insights from the CESM Large Ensemble. *Global Biogeochem. Cycles* **32**: 752–768. doi:[10.1029/2017GB005816](https://doi.org/10.1029/2017GB005816)
- Froneman, P. W., E. A. Pakhomov, and M. G. Balarin. 2004. Size-fractionated phytoplankton biomass, production and biogenic carbon flux in the eastern Atlantic sector of the Southern Ocean in late austral summer 1997–1998. *Deep-Sea Res. Part II Top. Stud. Oceanogr.* **51**: 2715–2729. doi:[10.1016/j.dsr2.2002.09.001](https://doi.org/10.1016/j.dsr2.2002.09.001)
- García, N. S., P. N. Sedwick, and G. R. DiTullio. 2009. Influence of irradiance and iron on the growth of colonial *Phaeocystis antarctica*: Implications for seasonal bloom dynamics in the Ross Sea, Antarctica. *Aquat. Microb. Ecol.* **57**: 203–220. doi:[10.3354/ame01334](https://doi.org/10.3354/ame01334)
- García-Muñoz, C., L. M. Lubián, C. M. García, Á. Marrero-Díaz, P. Sangrà, and M. Vernet. 2013. A mesoscale study of phytoplankton assemblages around the South Shetland Islands (Antarctica). *Polar Biol.* **36**: 1107–1123. doi:[10.1007/s00300-013-1333-5](https://doi.org/10.1007/s00300-013-1333-5)

- Gast, R. J., M. R. Dennett, and D. A. Caron. 2004. Characterization of protistan assemblages in the Ross Sea, Antarctica, by denaturing gradient gel electrophoresis. *Appl. Environ. Microbiol.* **70**: 2028–2037. doi:[10.1128/AEM.70.4.2028-2037.2004](https://doi.org/10.1128/AEM.70.4.2028-2037.2004)
- Georges, C., S. Monchy, S. Genitsaris, and U. Christaki. 2014. Protist community composition during early phytoplankton blooms in the naturally iron-fertilized Kerguelen area (Southern Ocean). *Biogeosciences* **11**: 5847–5863. doi:[10.5194/bg-11-5847-2014](https://doi.org/10.5194/bg-11-5847-2014)
- Gomi, Y., M. Fukuchi, and A. Taniguchi. 2010. Diatom assemblages at subsurface chlorophyll maximum layer in the eastern Indian sector of the Southern Ocean in summer. *J. Plankton Res.* **32**: 1039–1050. doi:[10.1093/plankt/fbq031](https://doi.org/10.1093/plankt/fbq031)
- Guillou, L., and others. 2013. The Protist Ribosomal Reference database (PR2): A catalog of unicellular eukaryote small sub-unit rRNA sequences with curated taxonomy. *Nucleic Acids Res.* **41**: D597–D604. doi:[10.1093/nar/gks1160](https://doi.org/10.1093/nar/gks1160)
- Hansen, B., P. K. Bjornsen, and P. J. Hansen. 1994. The size ratio between planktonic predators and their prey. *Limnol. Oceanogr.* **39**: 395–403. doi:[10.4319/lo.1994.39.2.0395](https://doi.org/10.4319/lo.1994.39.2.0395)
- Hashihama, F., T. Hirawake, S. Kudoh, J. Kanda, K. Furuya, Y. Yamaguchi, and T. Ishimaru. 2008. Size fraction and class composition of phytoplankton in the Antarctic marginal ice zone along the 140°E meridian during February–March 2003. *Polar Sci.* **2**: 109–120. doi:[10.1016/j.polar.2008.05.001](https://doi.org/10.1016/j.polar.2008.05.001)
- Higgins, H. W., S. W. Wright, and L. Schluter. 2011. Quantitative interpretation of chemotaxonomic pigment data, p. 257–313. *In* *Phytoplankton pigments: Characterization, chemotaxonomy and applications in oceanography*. Cambridge Univ. Press.
- Higgins, H. W., S. W. Wright, and L. Schlüter. 2011. Quantitative interpretation of chemotaxonomic pigment data, p. 257–313. *In* C. A. Llewellyn, E. S. Egeland, G. Johnsen, and S. Roy [eds.], *Phytoplankton Pigments: Characterization, chemotaxonomy and applications in oceanography*. Cambridge University Press.
- Hoffmann, L. J., I. Peeken, and K. Lochte. 2008. Iron, silicate, and light co-limitation of three Southern Ocean diatom species. *Polar Biol.* **31**: 1067–1080. doi:[10.1007/s00300-008-0448-6](https://doi.org/10.1007/s00300-008-0448-6)
- Holmes, R. M., A. Aminot, R. Kérouel, B. A. Hooker, and B. J. Peterson. 1999. A simple and precise method for measuring ammonium in marine and freshwater ecosystems. *Can. J. Fish. Aquat. Sci.* **56**: 1801–1808.
- Iida, T., and T. Odate. 2014. Seasonal variability of phytoplankton biomass and composition in the major water masses of the Indian Ocean sector of the Southern Ocean. *Polar Sci.* **8**: 283–297. doi:[10.1016/j.polar.2014.03.003](https://doi.org/10.1016/j.polar.2014.03.003)
- Irwin, A. J., Z. V. Finkel, O. M. E. Schofield, and P. G. Falkowski. 2006. Scaling-up from nutrient physiology to the size-structure of phytoplankton communities. *J. Plankton Res.* **28**: 459–471. doi:[10.1093/plankt/fbi148](https://doi.org/10.1093/plankt/fbi148)
- Johnston, T. M. S., and D. L. Rudnick. 2009. Observations of the transition layer. *J. Phys. Oceanogr.* **39**: 780–797. doi:[10.1175/2008JPO3824.1](https://doi.org/10.1175/2008JPO3824.1)
- Katoh, K., and D. M. Standley. 2013. MAFFT multiple sequence alignment software version 7: Improvements in performance and usability. *Mol. Biol. Evol.* **30**: 772–780. doi:[10.1093/molbev/mst010](https://doi.org/10.1093/molbev/mst010)
- Koch, F., S. Beszteri, L. Harms, and S. Trimborn. 2019. The impacts of iron limitation and ocean acidification on the cellular stoichiometry, photophysiology, and transcriptome of *Phaeocystis antarctica*. *Limnol. Oceanogr.* **64**: 357–375. doi:[10.1002/lno.11045](https://doi.org/10.1002/lno.11045)
- Kopczyńska, E. E., M. Fiala, and C. Jeandel. 1998. Annual and interannual variability in phytoplankton at a permanent station off Kerguelen Islands, Southern Ocean. *Polar Biol.* **20**: 342–351. doi:[10.1007/s003000050312](https://doi.org/10.1007/s003000050312)
- Kopczynska, E. E., F. Dehairs, M. Elskens, and S. Wright. 2001. Phytoplankton and microzooplankton variability between the Subtropical and Polar Fronts south of Australia: Thriving under regenerative and new production in late summer. *J. Geophys. Res. Oceans* **106**: 31597–31609. doi:[10.1029/2000JC000278](https://doi.org/10.1029/2000JC000278)
- Korb, R. E., M. J. Whitehouse, A. Atkinson, and S. E. Thorpe. 2008. Magnitude and maintenance of the phytoplankton bloom at South Georgia: A naturally iron-replete environment. *Mar. Ecol. Prog. Ser.* **368**: 75–91. doi:[10.3354/meps07525](https://doi.org/10.3354/meps07525)
- Landry, M. R., and others. 2002. Seasonal dynamics of phytoplankton in the Antarctic Polar Front region at 170°W. *Deep-Sea Res. Part II Top. Stud. Oceanogr.* **49**: 1843–1865. doi:[10.1016/S0967-0645\(02\)00015-2](https://doi.org/10.1016/S0967-0645(02)00015-2)
- Landry, M. R., K. E. Selph, A. G. Taylor, M. Décima, W. M. Balch, and R. R. Bidigare. 2011. Phytoplankton growth, grazing and production balances in the HNLC equatorial Pacific. *Deep-Sea Res. Part II Top. Stud. Oceanogr.* **58**: 524–535. doi:[10.1016/j.dsr2.2010.08.011](https://doi.org/10.1016/j.dsr2.2010.08.011)
- Lasbleiz, M., K. Leblanc, S. Blain, J. Ras, V. Cornet-Barthaux, S. Hélias Nunige, and B. Quéguiner. 2014. Pigments, elemental composition (C, N, P, and Si), and stoichiometry of particulate matter in the naturally iron fertilized region of Kerguelen in the Southern Ocean. *Biogeosciences* **11**: 5931–5955. doi:[10.5194/bg-11-5931-2014](https://doi.org/10.5194/bg-11-5931-2014)
- Lasbleiz, M., K. Leblanc, L. K. Armand, U. Christaki, C. Georges, I. Obernosterer, and B. Quéguiner. 2016. Composition of diatom communities and their contribution to plankton biomass in the naturally iron-fertilized region of Kerguelen in the Southern Ocean. *FEMS Microbiol. Ecol.* **92**: 1–16. doi:[10.1093/femsec/fiw171](https://doi.org/10.1093/femsec/fiw171)
- Laurenceau-Cornec, E. C., and others. 2015. The relative importance of phytoplankton aggregates and zooplankton fecal pellets to carbon export: Insights from free-drifting sediment trap deployments in naturally iron-fertilised waters near the Kerguelen Plateau. *Biogeosciences* **12**: 1007–1027. doi:[10.5194/bg-12-1007-2015](https://doi.org/10.5194/bg-12-1007-2015)

- Le Moigne, F. A. C., and others. 2016. What causes the inverse relationship between primary production and export efficiency in the Southern Ocean? *Geophys. Res. Lett.* **43**: 4457–4466. doi:10.1002/2016GL068480
- Lê, S., J. Josse, and F. Husson. 2008. FactoMineR: An R package for multivariate analysis. *J. Stat. Softw.* **25**: 1–18.
- Leynaert, A., E. Bucciarelli, P. Claquin, R. C. Dugdale, V. Martin-Jézéquel, P. Pondaven, and O. Ragueneau. 2004. Effect of iron deficiency on diatom cell size and silicic acid uptake kinetics. *Limnol. Oceanogr.* **49**: 1134–1143. doi:10.4319/lo.2004.49.4.1134
- Litchman, E., C. A. Klausmeier, O. M. Schofield, and P. G. Falkowski. 2007. The role of functional traits and trade-offs in structuring phytoplankton communities: Scaling from cellular to ecosystem level. *Ecol. Lett.* **10**: 1170–1181. doi:10.1111/j.1461-0248.2007.01117.x
- Love, M. I., W. Huber, and S. Anders. 2014. Moderated estimation of fold change and dispersion for RNA-seq data with DESeq2. *Genome Biol.* **15**: 550. doi:10.1186/s13059-014-0550-8
- Lovejoy, C., and others. 2007. Distribution, phylogeny, and growth of cold-adapted picoprasinophytes in Arctic Seas. *J. Phycol.* **43**: 78–89. doi:10.1111/j.1529-8817.2006.00310.x
- Lozupone, C., M. E. Lladser, D. Knights, J. Stombaugh, and R. Knight. 2011. UniFrac: An effective distance metric for microbial community comparison. *ISME J.* **5**: 169–172. doi:10.1038/ismej.2010.133
- Mackey, M. D., D. J. Mackey, H. W. Higgins, and S. W. Wright. 1996. CHEMTAX—a program for estimating class abundances from chemical markers: Application to HPLC measurements of phytoplankton. *Mar. Ecol. Prog. Ser.* **144**: 265–283.
- Maiti, K., M. A. Charette, K. O. Buesseler, and M. Kahru. 2013. An inverse relationship between production and export efficiency in the Southern Ocean. *Geophys. Res. Lett.* **40**: 1557–1561. doi:10.1002/grl.50219
- Marañón, E., P. M. Holligan, R. Barciela, N. González, B. Mouriño, M. J. Pazó, and M. Varela. 2001. Patterns of phytoplankton size structure and productivity in contrasting open-ocean environments. *Mar. Ecol. Prog. Ser.* **216**: 43–56. doi:10.3354/meps216043
- Marchetti, A., and N. Cassar. 2009. Diatom elemental and morphological changes in response to iron limitation: A brief review with potential paleoceanographic applications. *Geobiology* **7**: 419–431. doi:10.1111/j.1472-4669.2009.00207.x
- Marchetti, A., and others. 2009. Ferritin is used for iron storage in bloom-forming marine pennate diatoms. *Nature* **457**: 467–470. doi:10.1038/nature07539
- Marie, D., F. Partensky, D. Vaultot, and C. Brussaard. 1999. Enumeration of phytoplankton, bacteria, and viruses in marine samples. *Curr. Protoc. Cytom.* **10**: 11.11.1–11.11.15. doi:10.1002/0471142956.cy1111s10
- Martin, J. H. 1990. Glacial-interglacial CO₂ change: The iron hypothesis. *Paleoceanography* **5**: 1–13. doi:10.1029/PA005i001p00001
- Martin, P., J. T. Allen, M. J. Cooper, D. G. Johns, R. S. Lampitt, R. Sanders, and D. A. H. Teagle. 2010. Sedimentation of acantharian cysts in the Iceland Basin: Strontium as a ballast for deep ocean particle flux, and implications for acantharian reproductive strategies. *Limnol. Oceanogr.* **55**: 604–614. doi:10.4319/lo.2010.55.2.0604
- Martin, P., and others. 2013. Iron fertilization enhanced net community production but not downward particle flux during the Southern Ocean iron fertilization experiment LOHAFEX. *Global Biogeochem. Cycles* **27**: 871–881. doi:10.1002/gbc.20077
- McCarthy, J. 1981. The kinetics of nutrient utilization. *Can. Bull. Fish. Aquat. Sci.* **210**: 211–233.
- McMurdie, P. J., and S. Holmes. 2013. Phyloseq: An R package for reproducible interactive analysis and graphics of microbiome census data. *PLoS One* **8**: e61217. doi:10.1371/journal.pone.0061217
- Michaels, A. F., and M. W. Silver. 1988. Primary production, sinking fluxes and the microbial food web. *Deep-Sea Res. A* **35**: 473–490. doi:10.1016/0198-0149(88)90126-4
- Moline, M. A., B. B. Prezelin, O. Schofield, and R. C. Smith. 1996. Temporal dynamics of coastal Antarctic phytoplankton: Environmental driving forces and impact of 1991/92 summer diatom bloom on the nutrient regimes.
- Moline, M. A., B. B. Prezelin, O. Schofield, and R. C. Smith. 1997. Temporal dynamics of coastal Antarctic phytoplankton: Environmental driving forces and impact of a 1991/92 summer diatom bloom on the nutrient regimes., p. 67–72. *In* B. Battaglia, H. Valencia, and D. Walton [eds.], *Antarctic communities: Species, structure and survival*. Cambridge University Press.
- Mongin, M., E. Molina, and T. W. Trull. 2008. Seasonality and scale of the Kerguelen plateau phytoplankton bloom: A remote sensing and modeling analysis of the influence of natural iron fertilization in the Southern Ocean. *Deep-Sea Res. Part II Top. Stud. Oceanogr.* **55**: 880–892. doi:10.1016/j.dsr2.2007.12.039
- Moore, J. K., and M. R. Abbott. 2000. Phytoplankton chlorophyll distributions and primary production in the Southern Ocean. *J. Geophys. Res. Oceans* **105**: 28709–28722. doi:10.1029/1999JC000043
- Mosseri, J., B. Quéguiner, L. Armand, and V. Cornet-Barthaux. 2008. Impact of iron on silicon utilization by diatoms in the Southern Ocean: A case study of Si/N cycle decoupling in a naturally iron-enriched area. *Deep-Sea Res. Part II Top. Stud. Oceanogr.* **55**: 801–819. doi:10.1016/j.dsr2.2007.12.003
- Murtagh, F., and P. Legendre. 2014. Ward's hierarchical agglomerative clustering method: Which algorithms implement Ward's criterion? *J. Classif.* **31**: 274–295. doi:10.1007/s00357-014-9161-z

- Nuester, J., S. Vogt, and B. S. Twining. 2012. Localization of iron within centric diatoms of the genus *Thalassiosira*. *J. Phycol.* **48**: 626–634. doi:10.1111/j.1529-8817.2012.01165.x
- Oksanen, J., and others. 2017. vegan: Community ecology package. R package version 2.3-0.2015.
- Pauthenet, E., et al. 2018. Seasonal meandering of the polar front upstream of the kerguelen plateau. *Geophysical Research Letters*. **45**: 9774–9781. doi:10.1029/2018GL079614
- Park, Y.-H., F. Roquet, I. Durand, and J.-L. Fuda. 2008. Large-scale circulation over and around the Northern Kerguelen Plateau. *Deep-Sea Res. Part II Top. Stud. Oceanogr.* **55**: 566–581. doi:10.1016/j.dsr2.2007.12.030
- Pedrós-Alió, C. 2007. Dipping into the rare biosphere. *Science*. **315**: 192–193. doi:10.1126/science.1135933
- Peers, G., and N. M. Price. 2006. Copper-containing plastocyanin used for electron transport by an oceanic diatom. *Nature* **441**: 341–344. doi:10.1038/nature04630
- Penna, A. D., T. W. Trull, S. Wotherspoon, S. D. Monte, C. R. Johnson, and F. d'Ovidio. 2018. Mesoscale variability of conditions favoring an iron-induced diatom bloom downstream of the Kerguelen Plateau. *J. Geophys. Res. Oceans* **123**: 3355–3367. doi:10.1029/2018JC013884
- Piquet, A. M.-T., H. Bolhuis, M. P. Meredith, and A. G. J. Buma. 2011. Shifts in coastal Antarctic marine microbial communities during and after melt water-related surface stratification. *FEMS Microbiol. Ecol.* **76**: 413–427. doi:10.1111/j.1574-6941.2011.01062.x
- Planchon, F., and others. 2015. Carbon export in the naturally iron-fertilized Kerguelen area of the Southern Ocean based on the ²³⁴Th approach. *Biogeosciences* **12**: 3831–3848. doi:10.5194/bg-12-3831-2015
- Pollard, R. T., and others. 2009. Southern Ocean deep-water carbon export enhanced by natural iron fertilization. *Nature* **457**: 577–580. doi:10.1038/nature07716
- Price, M. N., P. S. Dehal, and A. P. Arkin. 2009. FastTree: Computing large minimum evolution trees with profiles instead of a distance matrix. *Mol. Biol. Evol.* **26**: 1641–1650. doi:10.1093/molbev/msp077
- Quéguiner, B., S. Blain, and T. Trull. 2007. High primary production and vertical export of carbon over the Kerguelen Plateau as a consequence of natural iron fertilization in a high-nutrient, low-chlorophyll environment, p. 167–172. *In* Proceedings of the The Kerguelen Plateau: Marine ecosystem and fisheries, Proceedings of the 1st international Science Symposium on the Kerguelen Plateau, Société Française d'Ichtyologie. Apr 14-16, 2010, Concarneau.
- R Core Team. 2018. R: A language and environment for statistical computing. R Foundation for Statistical Computing.
- Ras, J., H. Claustre, and J. Uitz. 2008. Spatial variability of phytoplankton pigment distributions in the Subtropical South Pacific Ocean: Comparison between in situ and predicted data. *Biogeosciences* **5**: 353–369. doi:10.5194/bg-5-353-2008
- Raven, J. A., B. Wollenweber, and L. L. Handley. 1992. A comparison of ammonium and nitrate as nitrogen sources for photolithotrophs. *New Phytol.* **121**: 19–32. doi:10.1111/j.1469-8137.1992.tb01088.x
- Reigstad, M., and P. Wassmann. 2007. Does *Phaeocystis* spp. contribute significantly to vertical export of organic carbon? p. 217–234. *In* M. A. Van Leeuwe, J. Stefels, S. Belviso, C. Lancelot, P. G. Verity, and W. W. C. Gieskes [eds.], *Phaeocystis*, major link in the biogeochemical cycling of climate-relevant elements. Springer.
- Rembauville, M., S. Blain, L. Armand, B. Quéguiner, and I. Salter. 2015. Export fluxes in a naturally iron-fertilized area of the Southern Ocean – part 2: Importance of diatom resting spores and faecal pellets for export. *Biogeosciences* **12**: 3171–3195. doi:10.5194/bg-12-3171-2015
- Rembauville, M., and others. 2017. Plankton assemblage estimated with BGC-Argo floats in the Southern Ocean: Implications for seasonal successions and particle export. *J. Geophys. Res. Oceans* **122**: 8278–8292. doi:10.1002/2017JC013067
- Rembauville, M., I. Salter, F. Dehairs, J.-C. Miquel, and S. Blain. 2018. Annual particulate matter and diatom export in a high nutrient, low chlorophyll area of the Southern Ocean. *Polar Biol.* **41**: 25–40. doi:10.1007/s00300-017-2167-3
- Richardson, T. L. 2018. Mechanisms and pathways of small-phytoplankton export from the surface ocean. *Ann. Rev. Mar. Sci.* **11**: 57–74. doi:10.1146/annurev-marine-121916-063627
- Richardson, T. L., and G. A. Jackson. 2007. Small phytoplankton and carbon export from the surface ocean. *Science* **315**: 838–840. doi:10.1126/science.1133471
- Schoemann, V., S. Becquevort, J. Stefels, V. Rousseau, and C. Lancelot. 2005. *Phaeocystis* blooms in the global ocean and their controlling mechanisms: A review. *J. Sea Res.* **53**: 43–66. doi:10.1016/j.seares.2004.01.008
- Schulz, I., and others. 2018. Remarkable structural resistance of a nanoflagellate-dominated plankton community to iron fertilization during the Southern Ocean experiment LOHAFEX. *Mar. Ecol. Prog. Ser.* **601**: 77–95. doi:10.3354/meps12685
- Sherr, E. B., and B. F. Sherr. 2007. Heterotrophic dinoflagellates: A significant component of microzooplankton biomass and major grazers of diatoms in the sea. *Mar. Ecol. Prog. Ser.* **352**: 187–197. doi:10.3354/meps07161
- Smetacek, V., P. Assmy, and J. Henjes. 2004. The role of grazing in structuring Southern Ocean pelagic ecosystems and biogeochemical cycles. *Antarct. Sci.* **16**: 541–558. doi:10.1017/S0954102004002317
- Smetacek, V., R. Scharek, and E.-M. Nöthig. 1990. Seasonal and Regional Variation in the Pelagial and its Relationship

- to the Life History Cycle of Krill. Antarctic Ecosystems. Springer Berlin Heidelberg. 103–114.
- Smith, W. O., M. R. Dennett, S. Mathot, and D. A. Caron. 2003. The temporal dynamics of the flagellated and colonial stages of *Phaeocystis antarctica* in the Ross Sea. Deep-Sea Res. Part II Top. Stud. Oceanogr. **50**: 605–617. doi:10.1016/S0967-0645(02)00586-6
- Sekagiri, A., W. Sloan, and U. Ijaz. 2018. microbiomeSeq: An R package for microbial community analysis in an environmental context. Available from <http://www.github.com/umerijaz/microbiomeSeq>
- Swanberg, N. R., and D. A. Caron. 1991. Patterns of sarcodine feeding in epipelagic oceanic plankton. J. Plankton Res. **13**: 287–312. doi:10.1093/plankt/13.2.287
- Tang, K. W., W. O. Smith Jr., D. T. Elliott, and A. R. Shields. 2008. Colony size of *Phaeocystis antarctica* (prymnesiophyceae) as influenced by zooplankton grazers. J. Phycol. **44**: 1372–1378. doi:10.1111/j.1529-8817.2008.00595.x
- Thiele, S., C. Wolf, I. K. Schulz, P. Assmy, K. Metfies, and B. M. Fuchs. 2014. Stable composition of the nano- and picoplankton community during the ocean iron fertilization experiment LOHAFEX. PLoS One **9**: e113244. doi:10.1371/journal.pone.0113244
- Timmermans, K. R., B. van der Wagt, M. J. W. Veldhuis, A. Maatman, and H. J. W. de Baar. 2005. Physiological responses of three species of marine pico-phytoplankton to ammonium, phosphate, iron and light limitation. J. Sea Res. **53**: 109–120. doi:10.1016/j.seares.2004.05.003
- Uitz, J., H. Claustre, F. B. Griffiths, J. Ras, N. Garcia, and V. Sandroni. 2009. A phytoplankton class-specific primary production model applied to the Kerguelen Islands region (Southern Ocean). Deep-Sea Res. Part I Oceanogr. Res. Pap. **56**: 541–560. doi:10.1016/j.dsr.2008.11.006
- Uitz, J., H. Claustre, B. Gentili, and D. Stramski. 2010. Phytoplankton class-specific primary production in the world's oceans: Seasonal and interannual variability from satellite observations. Global Biogeochem. Cycles. **24**: 1–19. doi:10.1029/2009GB003680
- Van Heukelem, L., and C. S. Thomas. 2001. Computer-assisted high-performance liquid chromatography method development with applications to the isolation and analysis of phytoplankton pigments. J. Chromatogr. A **910**: 31–49. doi:10.1016/S0378-4347(00)00603-4
- van Leeuwe, M. A., R. J. W. Visser, and J. Stefels. 2014. The pigment composition of *Phaeocystis antarctica* (Haptophyceae) under various conditions of light, temperature, salinity, and iron. J. Phycol. **50**: 1070–1080. doi:10.1111/jpy.12238
- Wang, Q., G. M. Garrity, J. M. Tiedje, and J. R. Cole. 2007. Naïve Bayesian classifier for rapid assignment of rRNA sequences into the new bacterial taxonomy. Appl. Environ. Microbiol. **73**: 5261–5267. doi:10.1128/AEM.00062-07
- Weber, L. H., and S. Z. El-Sayed. 1987. Contributions of the net, nano- and picoplankton to the phytoplankton standing crop and primary productivity in the Southern Ocean. J. Plankton Res. **9**: 973–994. doi:10.1093/plankt/9.5.973
- Wickham, H. 2011. ggplot2. Wiley Interdiscip. Rev. Comput. Stat. **3**: 180–185.
- Wickham, H. 2016. ggplot2: Elegant graphics for data analysis. Springer.
- Wolf, C., S. Frickenhaus, E. S. Kiliyas, I. Peeken, and K. Metfies. 2014. Protist community composition in the Pacific sector of the Southern Ocean during austral summer 2010. Polar Biol. **37**: 375–389. doi:10.1007/s00300-013-1438-x
- Wright, S. W., D. Thomas, H. Marchant, H. Higgins, M. Mackey, and D. Mackey. 1996. Analysis of phytoplankton of the Australian sector of the Southern Ocean: Comparisons of microscopy and size frequency data with interpretations of pigment HPLC data using the 'CHEMTAX' matrix factorisation program. Mar. Ecol. Prog. Ser. **144**: 285–298. doi:10.3354/meps144285
- Wright, S. W., A. Ishikawa, H. J. Marchant, A. T. Davidson, R. L. van den Eenden, and G. V. Nash. 2009. Composition and significance of picophytoplankton in Antarctic waters. Polar Biol. **32**: 797–808. doi:10.1007/s00300-009-0582-9
- Wright, S. W., R. L. van den Eenden, I. Pearce, A. T. Davidson, F. J. Scott, and K. J. Westwood. 2010. Phytoplankton community structure and stocks in the Southern Ocean (30–80 E) determined by CHEMTAX analysis of HPLC pigment signatures. Deep-Sea Res. Part II Top. Stud. Oceanogr. **57**: 758–778.

Acknowledgments

We thank B. Quéguiner, the PI of the MOBYDICK project, for providing us the opportunity to participate to this cruise, the captain, and crew of the R/V *Marion Dufresne* for their enthusiasm and support aboard during the MOBYDICK-THEMISTO cruise (<https://doi.org/10.17600/18000403>) and the chief scientist I. Obernosterer, whose valuable comments considerably improved this manuscript. This work was supported by the French oceanographic fleet (Flotte océanographique française), the French ANR ("Agence Nationale de la Recherche," AAPG 2017 program, MOBYDICK Project number: ANR-17-CE01-0013), and the French Research program of INSU-CNRS LEFE/CYBER ("Les enveloppes fluides et l'environnement"—"Cycles biogéochimiques, environnement et ressources"). We also thank the French Ministry of Higher Education and the Region des Hauts de France for funding the Ph.D. grant to S.I.

Conflict of Interest

None declared.

Submitted 17 January 2020

Revised 29 May 2020

Accepted 11 June 2020

Associate editor: Heidi Sosik